

AD/A-002 277

AN ITERATIVE APPROXIMATION TO THE MIXED-SIGNAL PROCESSOR.

R. R. Blandford, et al

Teledyne Geotech

Prepared for:

Defense Advanced Research Projects Agency
Air Force Technical Applications Center

23 October 1973

DISTRIBUTED BY:

NTIS

National Technical Information Service
U. S. DEPARTMENT OF COMMERCE

Unclassified

SECURITY CLASSIFICATION OF THIS PAGE (When Data Entered)

REPORT DOCUMENTATION PAGE		READ INSTRUCTIONS BEFORE COMPLETING FORM
1. REPORT NUMBER SDAC-TR-73-7	2. GOVT ACCESSION NO	3. RECIPIENT'S CATALOG NUMBER AD/A-002277
4. TITLE (and Subtitle) AN ITERATIVE APPROXIMATION TO THE MIXED-SIGNAL PROCESSOR		5. TYPE OF REPORT & PERIOD COVERED Technical
7. AUTHOR(s) Blandford, R. R., Cohen, T. J., and Woods, J. W.		6. PERFORMING ORG. REPORT NUMBER
9. PERFORMING ORGANIZATION NAME AND ADDRESS Teledyne Geotech 314 Montgomery Street Alexandria, Virginia 22314		8. CONTRACT OR GRANT NUMBER(s) F08606-74-C-0006
11. CONTROLLING OFFICE NAME AND ADDRESS Defense Advanced Research Projects Agency Nuclear Monitoring Research Office 1400 Wilson Blvd. Arlington, Va. 22209		10. PROGRAM ELEMENT PROJECT TASK AREA & WORK UNIT NUMBER
14. MONITORING AGENCY NAME & ADDRESS (if different from Controlling Office) Vela Seismological Center 312 Montgomery Street Alexandria, Virginia 22314		12. REPORT DATE 23 October 1973
		13. NUMBER OF PAGES 76
		15. SECURITY CLASS (of this report)
		15a. DECLASSIFICATION/DOWNGRADING SCHEDULE
16. DISTRIBUTION STATEMENT (of this Report) APPROVED FOR PUBLIC RELEASE; DISTRIBUTION UNLIMITED.		
17. DISTRIBUTION STATEMENT (of the abstract entered in Block 20, if different from Report)		
18. SUPPLEMENTARY NOTES Reproduced by NATIONAL TECHNICAL INFORMATION SERVICE US Department of Commerce Springfield, VA. 22151		
19. KEY WORDS (Continue on reverse side if necessary and identify by block number) Beam-forming Mixed-signal Analysis Maximum-likelihood estimation Iterative beam-forming		
20. ABSTRACT (Continue on reverse side if necessary and identify by block number) An iterative beam processor is developed which in the limit is identical to the mixed-signal processor (Dean et.al., 1968). Assuming that two events arrive simultaneously at an array consisting of N sensors, the array is first beamed on one of the two epicenters to produce a signal estimate for this event (0'th iteration). This signal estimate is then time-shifted and subtracted from each of the original N seismograms in an attempt to		

DDC
RECEIVED
DEC 20 1974
D

DD FORM 1 JAN 73 1473

EDITION OF 1 NOV 65 IS OBSOLETE

Unclassified

SECURITY CLASSIFICATION OF THIS PAGE (When Data Entered)

Unclassified

SECURITY CLASSIFICATION OF THIS PAGE (When Data Entered)

remove the signal from the original seismograms. The new set of records, each containing N stripped seismograms, is then beamed to produce a signal estimate for the second event. The signal estimate for the second event is now time-shifted, subtracted from the original N seismograms, and the stripped seismograms are rebeamed on the first event. The process is repeated until differences in successive signal estimates for the desired event fall below a predetermined threshold. The iterative-beam processor has great practical (and intuitive) appeal. For seven or more elements, the iterative process converges in a few iterations requiring only a few shift and sum operations per data point, while the equivalent mixed-signal (asymptotic maximum-likelihood) processor requires a convolution for each data point.

//

Unclassified

SECURITY CLASSIFICATION OF THIS PAGE (When Data Entered)

AN ITERATIVE APPROXIMATION TO THE MIXED-SIGNAL PROCESSOR

Seismic Data Analysis Center Report No.: SDAC-TR-73-7

AFTAC Project No.: VELA VT/4709
Project Title: Seismic Data Analysis Center
ARPA Order No.: 1620
ARPA Program Code No.: 3F10

Name of Contractor: TELEDYNE GEOTECH

Contract No.: F08606-74-C-0006
Date of Contract: 01 July 1973
Amount of Contract: \$2,152,172
Contract Expiration Date: 30 June 1974
Project Manager: Robert G. Van Nostrand
(703) 836-3882

P. O. Box 334, Alexandria, Virginia 22314

APPROVED FOR PUBLIC RELEASE; DISTRIBUTION UNLIMITED.

ABSTRACT

An iterative beam processor is developed which in the limit is identical to the mixed-signal processor (Dean et. al., 1968). Assuming that two events arrive simultaneously at an array consisting of N sensors, the array is first beamed on one of the two epicenters to produce a signal estimate for this event (0'th iteration). This signal estimate is then time-shifted and subtracted from each of the original N seismograms in an attempt to remove the signal from the original seismograms. The new set of records, each containing N stripped seismograms, is then beamed to produce a signal estimate for the second event. The signal estimate for the second event is now time-shifted, subtracted from the original N seismograms, and the stripped seismogram are rebeamed on the first event. The process is repeated until differences in successive signal estimates for the desired event fall below a predetermined threshold. The iterative-beam processor has great practical (and intuitive) appeal. For seven or more elements, the iterative process converges in a few iterations requiring only a few shift and sum operation per data point, while the equivalent mixed-signal (asymptotic maximum-likelihood) processor requires a convolution for each data point.

TABLE OF CONTENTS

	Page
ABSTRACT	
INTRODUCTION	1
SIGNAL ANALYSIS THEORY	3
RESULTS	8
Data	8
Demonstrations of the Mixed-Signals and Iterative Beam Processors	8
Characteristics of the Iterative-Beam Processor	20
Two-Signals- 7 Channels	20
Two Signals - 19 Channels	27
One Signal - 7 Channels	33
One Signal - 19 Channels	39
Noise	45
CONCLUSIONS	54
ACKNOWLEDGEMENTS	55
REFERENCES	56
APPENDIX I - Theoretical Proof of the Equi- lence of Iterative Two-Signal Beam- ing and Maximum-Likelihood Processing.	AI-1
APPENDIX II - Discussion of Bias in an Alterna- tive Iterative Signal Processor.	AII-1

LIST OF FIGURES

Figure No.	Figure Title	Page No.
1	Iterative-beam processor.	5
2	Array configuration for TFO.	9
3	Seismograms for the Fox Islands Event.	12
4	Seismograms for the Tonga Islands Event.	13
5	Superposition of the Tonga and Fox Islands Events.	14
6	Comparison of the beam, mixed-signal and iterative-beam processors using the superimposed Tonga and Fox Islands signals (7 channels).	15
7	Comparison of the beam, mixed-signal, and iterative-beam processors using the superimposed Tonga and Fox Islands signals (19 channels).	17
8	Comparison of the beam, mixed-signal and iterative-beam processors using the Fox Islands signal (19 channels).	19
9a	Convergence characteristics for the Tonga Islands iterative-beam signal estimates, superimposed Tonga and Fox Islands signals, 7 channels.	22
9b	Convergence characteristics for the Tonga Islands iterative-beam signal estimates, superimposed Tonga and Fox Islands signals, 7 channels, predictable bias removed.	22
10	Iterative-beam Tonga Islands signal estimates, superimposed Tonga and Fox Islands signals, 7 channels.	23

LIST OF FIGURES (continued)

Figure No.	Figure Title	Page No.
11a	Convergence characteristics for the Fox Islands iterative-beam signal estimates, superimposed Tonga and Fox Islands signals, 7 channels.	24
11b	Convergence characteristics for the Fox Islands iterative-beam signal estimates, Tonga and Fox Islands signals, predictable bias removed.	24
12	Iterative-beam Fox Islands signal estimates, superimposed Tonga and Fox Islands signals, 7 channels.	25
13	Convergence characteristics for the Tonga Islands iterative-beam signal estimates, superimposed Tonga and Fox Islands signals, 19 channels.	29
14	Iterative-beam Tonga Islands signal estimates, superimposed Tonga and Fox Islands signals, 19 channels.	30
15	Convergence characteristics for the Fox Islands iterative-beam signal estimates, superimposed Tonga and Fox Islands signals, 19 channels.	31
16	Iterative-beam Fox Islands signal estimates, factors, superimposed Tonga and Fox Islands signals, 19 channels.	32
17	Convergence characteristics for the Tonga Islands iterative-beam signal estimates, Fox Islands signal, 7 channels.	35

LIST OF FIGURES (Continued)

Figure No.	Figure Title	Page No.
18	Iterative-beam Tonga Islands signal estimates, Fox Islands signal, 7 channels.	36
19	Convergence characteristics for the Fox Islands iterative-beam signal estimates, Fox Islands signal, 7 channels.	37
20	Iterative-beam Fox Islands signal estimates, Fox Islands signal, 7 channels.	38
21	Convergence characteristics for the Tonga Islands iterative-beam signal estimates, Fox Islands signal, 19 channels.	41
22	Iterative-beam Tonga Islands signal estimates, Fox Islands signal, 19 channels.	42
23	Convergence characteristics for the Fox Islands iterative-beam signal estimates, Fox Islands signal, 19 channels.	43
24	Iterative-beam Fox Islands signal estimates, Fox Islands signal, 19 channels.	44
25	Comparison of noise estimates from noise recorded prior to the arrival of the Fox Islands signal, 7 channels.	47
26	Comparison of noise estimates from noise recorded prior to the arrival of the Fox Islands signal, 19 channels.	48

LIST OF TABLES

Table No.	Table Title	Page No.
I	Coordinates of TFO Instruments (Z-1 thru Z-19)	10
II	Earthquake Source Data	11
III	Iterative-Beam Analysis, Two Signals, 7 Channels	21
IV	Iterative-Beam Analysis, Two Signals, 19 Channels	28
V	Iterative-Beam Analysis, One Signal, 7 Channels	34
VI	Iterative-Beam Analysis, One Signal, 19 Channels	40
VII	Iterative-Beam Analysis, Noise(Fox Islands)	
	a. 7 Channels	45
	b. 19 Channels	46
VIII	Iterative-Beam Analysis, Noise(Tonga Islands)	
	a. 7 Channels	49
	b. 19 Channels	50
IX	Comparison of rms Noise Estimates	51

INTRODUCTION

The classical method for separating two signals which arrive simultaneously at a seismic array is to beam the array on each of the event epicenters. Unfortunately, the simple beam does not always yield satisfactory signal estimates due to contamination of one signal's estimate by leakage from the other signal. Shumway (1972), however, demonstrated that a mixed-signal (asymptotic maximum-likelihood) processor yields better signal estimates than does simple beamforming. Using various TFO subarrays, and superimposed signals from an earthquake in the Fox Islands and one in the Tonga Islands, Shumway found that the superiority of the mixed-signal processor was especially pronounced for small arrays. Similarly, Cohen (1972), in a study of the coda suppression capabilities of the beam and mixed-signal processors performed using signals recorded at TFO, found that the coda attenuation obtained using a 7-element subarray and the mixed-signal processor was comparable to that obtained using a 19-element subarray and the beam.

While the superiority of the mixed-signal processor has been established by these and other studies, it is not always practical to use the maximum-likelihood approach. A convolution is required for each data point; as such, when data from a large array with long moveouts must be processed, limitations on core and computational-time may prevent its use. The

iterative-beam approximation to the mixed-signal processor can overcome these drawbacks. Also, the iterative beamforming approach is similar in concept to simple beamforming and (by minimal investments in additional system programming) may be able to take advantage of existing hardware and software in operational systems.

In this report we first introduce the iterative-beam processor, and demonstrate both theoretically and empirically that in the limit it yields results identical to those produced by the mixed-signal processor. We next determine the characteristics of the iterative-beam approximation, specifically inquiring into the rate of convergence. Finally, we examine the action of the iterative-beam processor on noise. Here, the data suggest that the iterative-beam processor (and hence the mixed-signal processor) behaves in a manner similar to that of the simple beam; that is, it reduces the rms levels of the final noise estimates by approximately $N^{1/2}$, where N is the number of sensors in the array.

SIGNAL ANALYSIS THEORY

Consider the collection of signals:

$$y_j(t) = \sum_{u=-\infty}^{\infty} \sum_{k=1}^p x_{jk}(t-u) s_k(u) + n_j(t) \quad (1)$$

where

$y_j(t)$, $j = 1, \dots, n$, is the collection of N observed time series; $s_k(t)$, $k = 1, \dots, p$, is the collection of signals to be estimated; $x_{jk}(t) = \delta(t - T_{jk})$ [where $\delta(t) = 1$ for $t = 0$, zero otherwise]; and $n_j(t)$ is the noise on the j 'th channel.

We assume that the signals can be estimated by linear estimates of the type:

$$s_k(t) = \sum_{j=1}^n \int_{-\infty}^{\infty} h_{kj}(\tau) y_j(t-\tau) d\tau \quad (2)$$

where $h_{kj}(\tau)$ is a $p \times n$ matrix of filter functions to be determined.

Using this formulation, Dean et. al., (1968) showed that in the frequency domain, and for uncorrelated noise, the matrix of filter coefficients which produces the best linear unbiased estimates of the $s_k(t)$ is given by

$$\hat{Y}(\omega) = [X^*(\omega) X(\omega)]^{-1} X^*(\omega) Y(\omega). \quad (3)$$

Transforming the $H(\omega)$ calculated at each frequency back into time, the signal estimates $\hat{s}_k(t)$ can then be obtained by convolving the filters with the $y_i(t)$. For a single signal ($k=1$) in uncorrelated noise, $\hat{s}_1(t)$ is the beam.

A block diagram of the iterative-beam processor is given in Figure 1. That this processor, in the limit as the number of iterations becomes large, yields results identical to those produced by the mixed-signal processor is shown in Appendix I. Briefly, with respect to Figure 1, we assume that signals from two events are recorded at an array consisting of N sensors. The array is first beamed on one of the two epicenters to produce a signal estimate for the chosen event. This estimate is then time-shifted and subtracted from each seismogram of the original N seismogram in an attempt to remove the given event's signal from the original seismograms. We now have a new set of array seismograms which contains primarily those signals corresponding to the second signal. This set, containing N stripped seismograms, is now beamed to produce a signal estimate for the second event. The subtraction and beaming process is repeated until, for example, the differences in successive signal estimates for the desired event falls below a pre-determined threshold.

The technique of stripping seismograms to enhance various arrivals is identical to the method of consecutive subtraction of coherent noise described by Passechnik (1972). Further, it is of interest to note

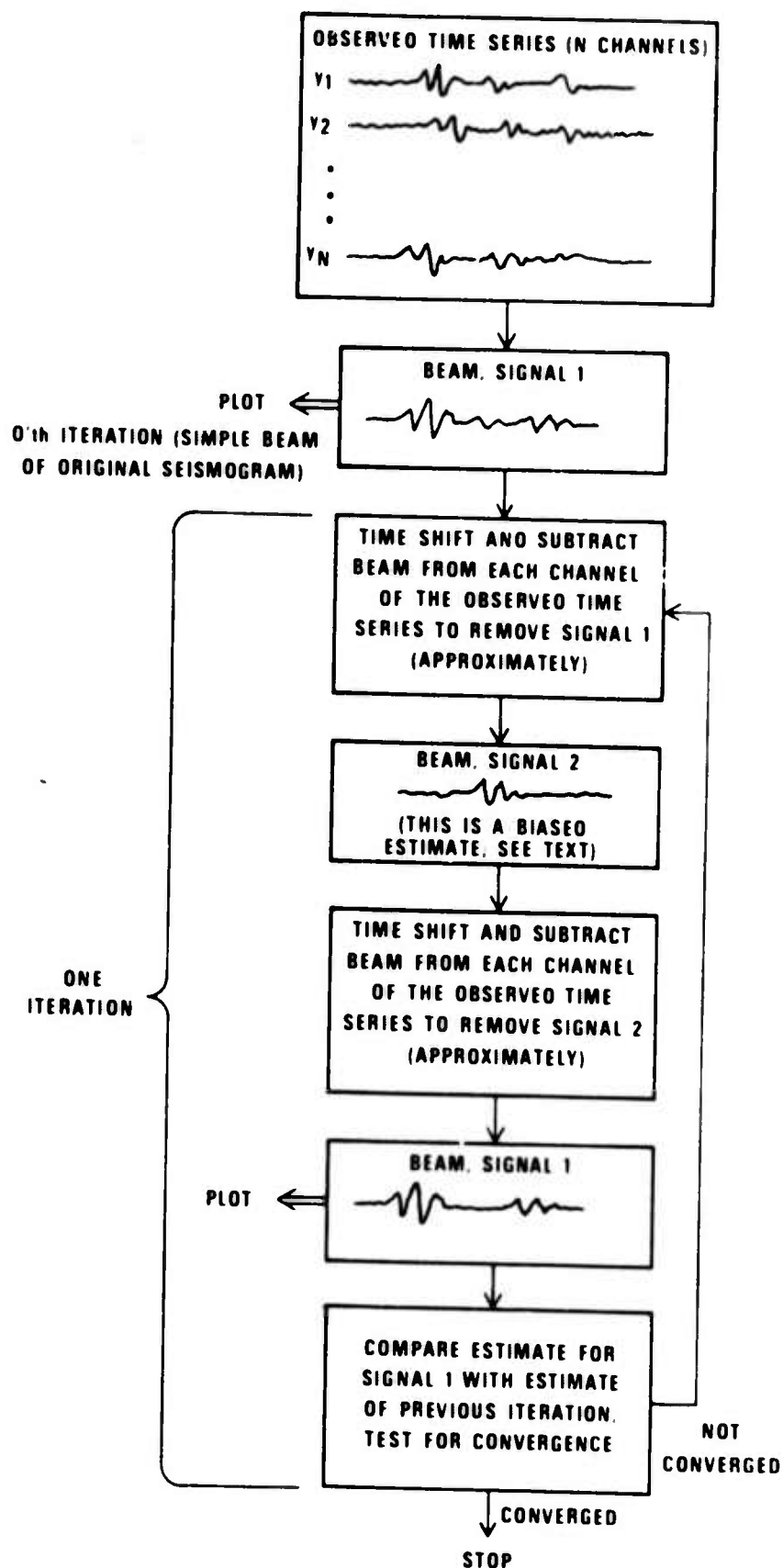


Figure 1. Iterative-beam processor.

that the "stripping" process discussed by Smart (1972) can be seen to be the first step in this iterative process, and thus to be a first approximation to a maximum-likelihood process.

There are actually two iterative methods for obtaining a signal estimate for a selected event. We can proceed as discussed previously, beaming first on the event for which we desire a signal estimate, and iterating according to the scheme shown in Figure 1. Alternatively, we can start by beaming on the second signal present (for which we may not desire a signal estimate), iterate according to the method of Figure 1, but take the signal estimates for the event of interest at the middle of each iteration. It should be noted, however, that the estimate of the signal extracted at the middle of an iteration is biased (see Appendix II for details).

In our analysis of the iterative beam processor corresponding signal amplitudes on each channel of the original seismograms are approximately equal. As such, we weight the beam estimates by the reciprocal of the number of channels summed. The iterative solution computed using equal weighting factors corresponds directly to the solution which would be obtained using the mixed-signal processor, since the signal model in these cases is given by:

$$y_j(t) = s_1(t - T_{j1}) + s_2(t - T_{j2}) + n_j(t)$$

where

$y_j(t)$, $j = 1, \dots, n$ is the collection of N observed time series; $s_1(t)$ and $s_2(t)$ are propagating plane waves; T_{j1} and T_{j2} are appropriate delay times for the j 'th sensor and $n_j(t)$ is the noise signal on the j 'th sensor.

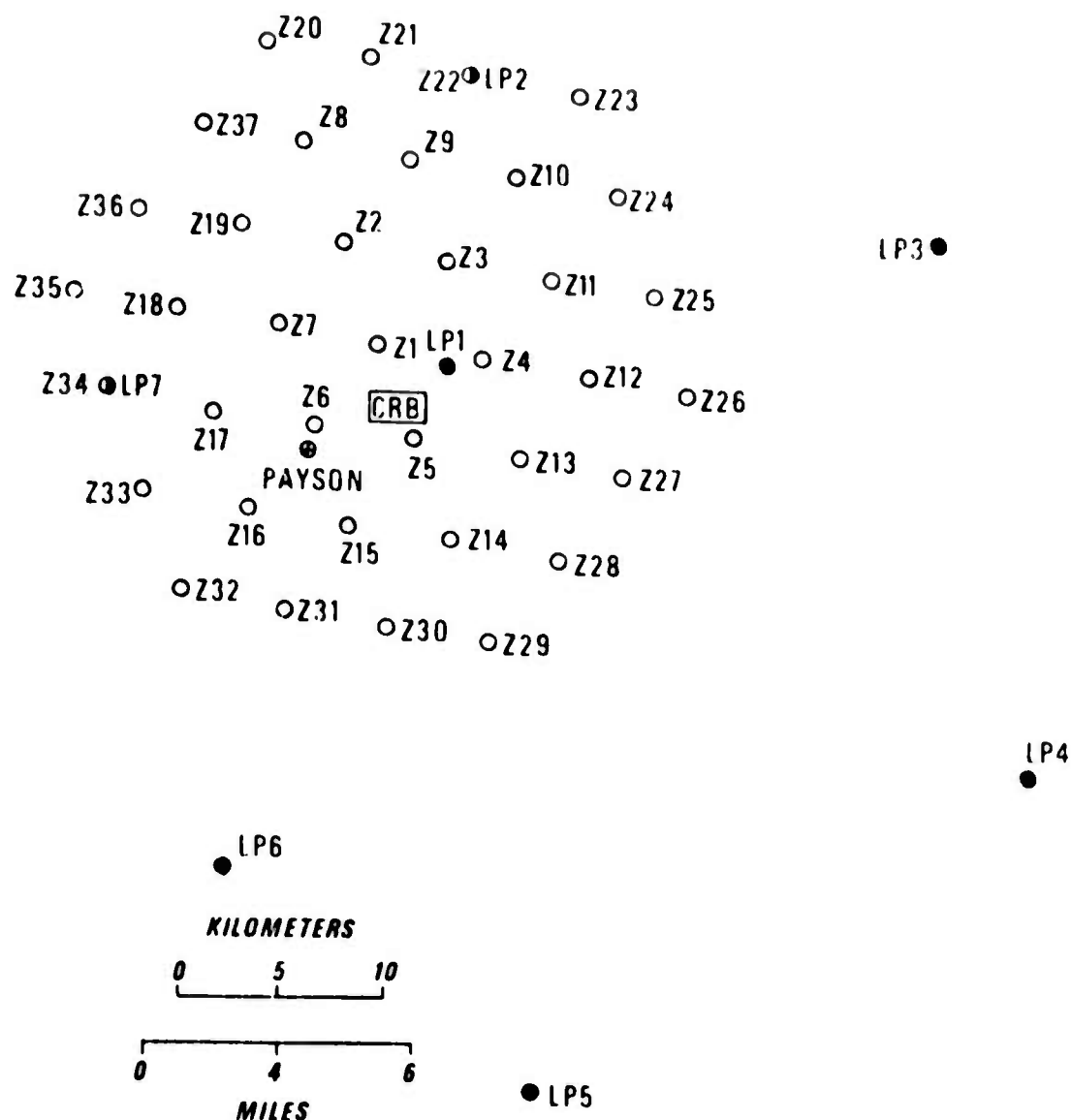
RESULTS

Data

Seismograms recorded at the inner 19 elements of TFO (Figure 2, Table I) for two events (Table II), one from the Fox Islands (Figure 3), and the other from the Tonga Islands (Figure 4), were used to investigate the characteristics and capabilities of the iterative-beam processor. Both events were recorded at each sensor with signal-to-noise ratios of 25 to 30 db. To simulate the near-simultaneous arrival of two events at TFO, seismograms for these events were superimposed; delays for the arrivals from the Fox Islands event relative to the arrivals from the Tonga Islands event were taken to be on the order of 4 to 5 seconds. Thus the composite data set (Figure 5) corresponds closely to the data used by Shumway (1972) to evaluate the mixed-signal processor.

Demonstrations of the Mixed-Signal and Iterative-Beam Processors

To demonstrate initially that the mixed-signal processor and iterative-beam processor with equal weights yield identical results, the processors were applied to the mixed-signal data shown in channels 1-7 of Figure 5. The results of the analyses are shown in Figure 6. As seen in Figures 6b and d, the signal estimates for both events obtained using the iterative-beam processor are virtually identical to



- ① THE ○ CIRCLES LABELED Z1 THROUGH Z37 ARE CENTERED ON THE 37 SHORT PERIOD SEISMOMETER LOCATIONS
- ② THE ● CIRCLES LABELED LP1 THROUGH LP7 ARE CENTERED ON THE 7 THREE - COMPONENT LONG PERIOD SEISMOMETERS
- ③ THE CRB IS THE CENTRAL RECORDING BUILDING

Figure 2. Array configuration for TFO.

TABLE I
Coordinates of TFO Instruments
Z1 - Z19
SHORT PERIOD

	<u>LATITUDE</u>	<u>LONGITUDE</u>	<u>ELEVATION (Meters)</u>
Z-1	34 16 42.3300N	111 18 12.2560W	1615.42
Z-2	34 19 14.1190N	111 19 26.6720W	1489.75
Z-3	34 18 42.5760N	111 16 56.0730W	1515.3
Z-4	34 16 13.8910N	111 14 56.7380W	1474.6
Z-5	34 14 10.2220N	111 17 2.2670W	1491.9
Z-6	34 14 55.6970N	111 20 7.0030W	1509.4
Z-7	34 17 9.1830N	111 21 24.5490W	1403.2
Z-8	34 21 42.2900N	111 20 23.5360W	1805.4
Z-9	34 21 10.0020N	111 17 12.9640W	1569.4
Z-10	34 20 52.2090N	111 14 4.9130W	1658.5
Z-11	34 18 4.8650N	111 12 23.8630W	1904.9
Z-12	34 15 49.5070N	111 11 44.7380W	1528.29
Z-13	34 13 48.4020N	111 13 48.3160W	1513.74
Z-14	34 11 41.4430N	111 16 30.2940W	1534.0
Z-15	34 12 8.0760N	111 19 8.4440W	1487.4
Z-16	34 12 32.0810N	111 22 13.9550W	1462.9
Z-17	34 15 3.9540N	111 23 28.2740W	1426.4
Z-18	34 17 40.8760N	111 24 39.9550W	1664.9
Z-19	34 19 39.8540N	111 22 32.4010W	1588.55

TABLE II
Earthquake Source Data

<u>REGION</u>	<u>DATE</u>	<u>LATITUDE</u>	<u>LONGITUDE</u>	<u>DEPTH (km)</u>	<u>m_b</u>	<u>ORIGIN TIME</u>	<u>DISTANCE TO TFO</u>
Fox Islands	24 Aug 69	52.5°N	168.6°W	33	5.2	00 46 14.6	44.7°
Tonga Islands	22 Jul 69	18.1°S	172.5°W	30	5.4	13 48 36.5	78.0°

FOX ISLANDS

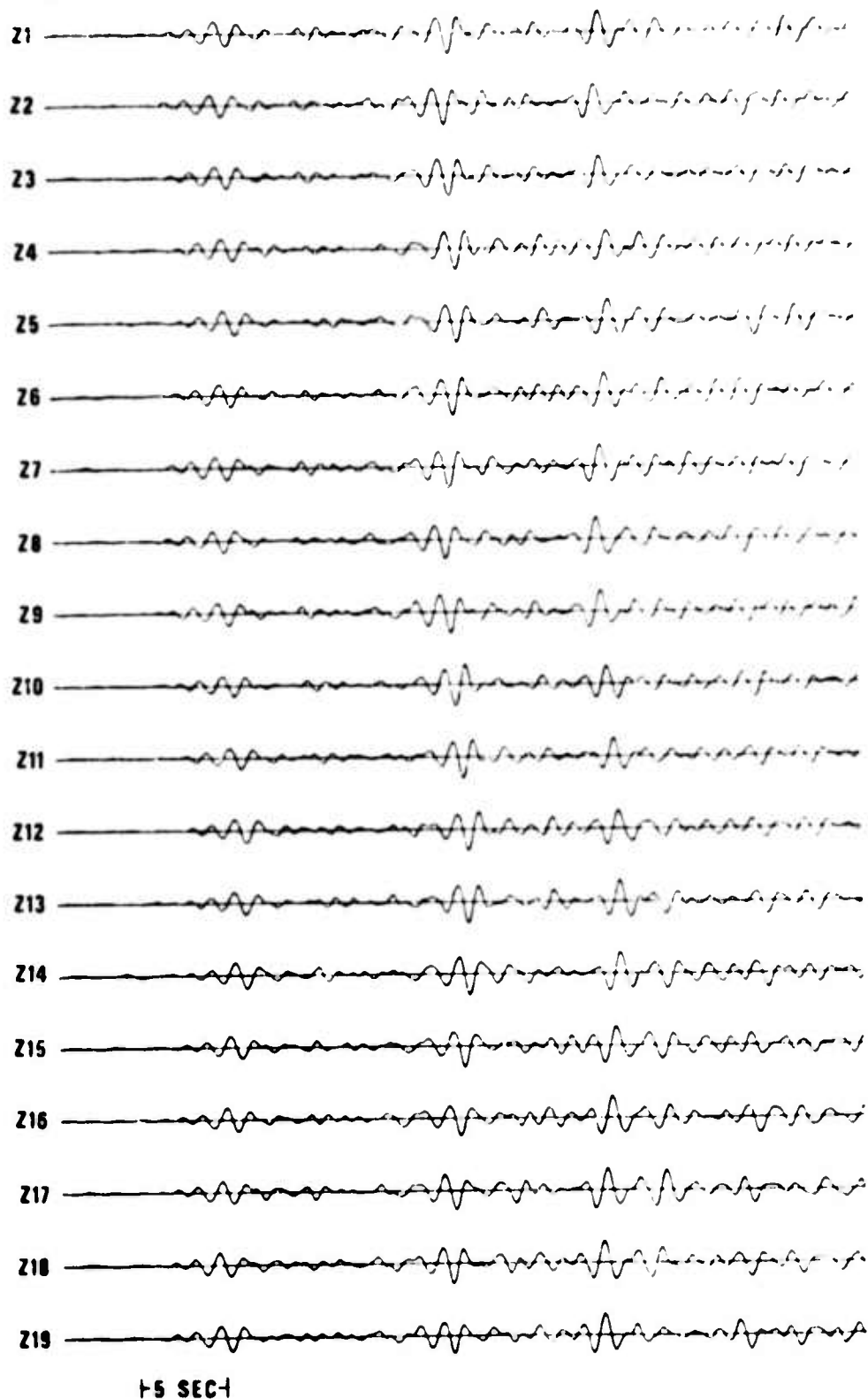


Figure 3. Seismograms for the Fox Islands Event.

TONGA ISLANDS

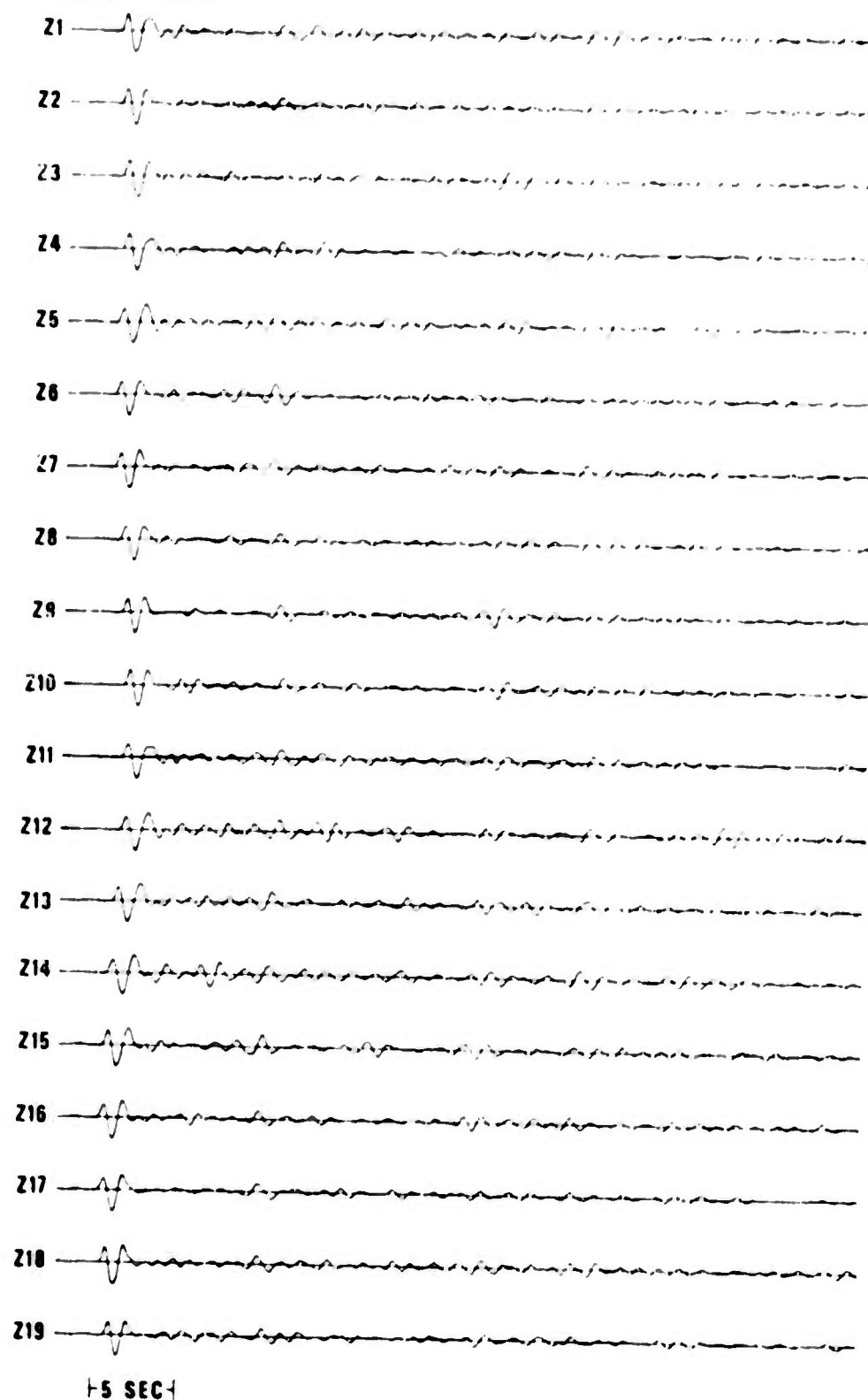


Figure 4. Seismograms for the Tonga Islands Event.

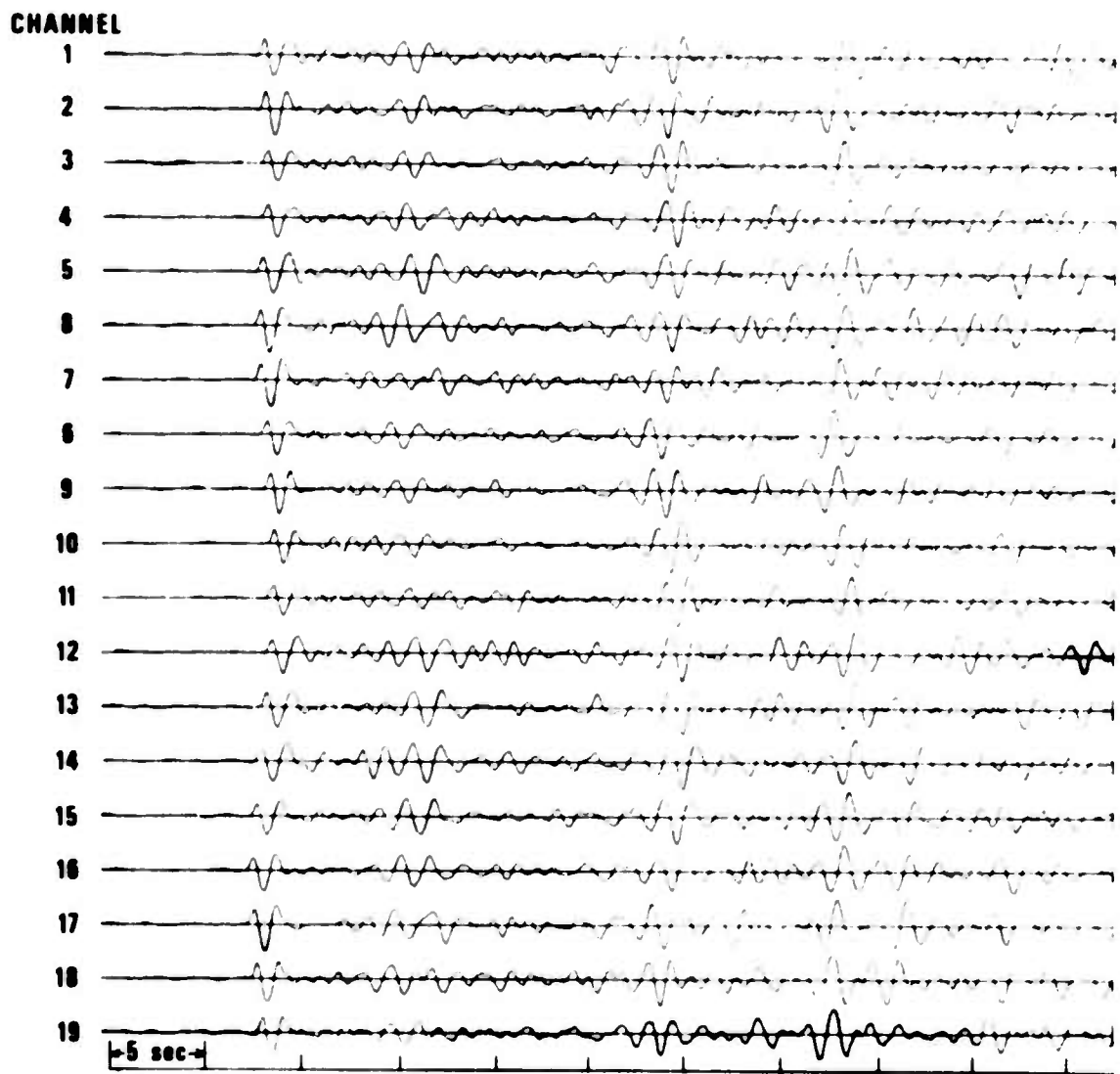


Figure 5. Superposition of the Tonga and Fox Islands Events.

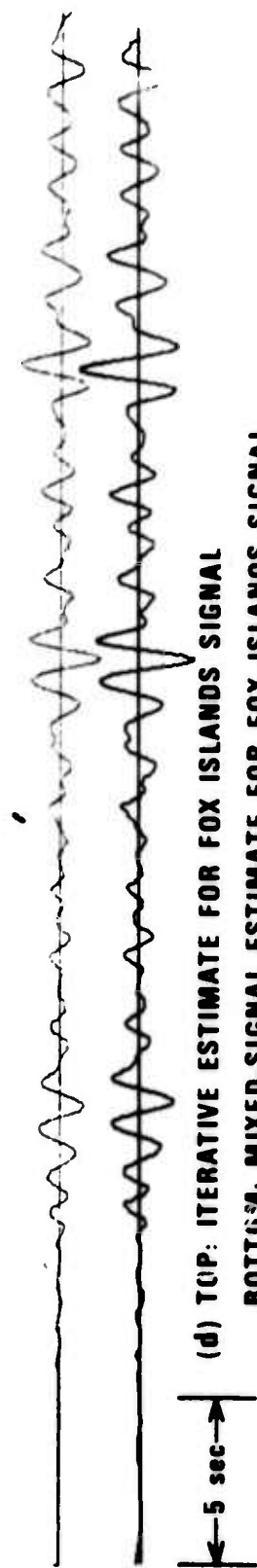
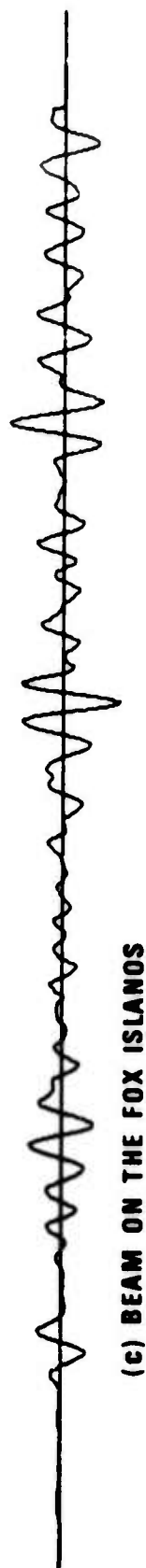
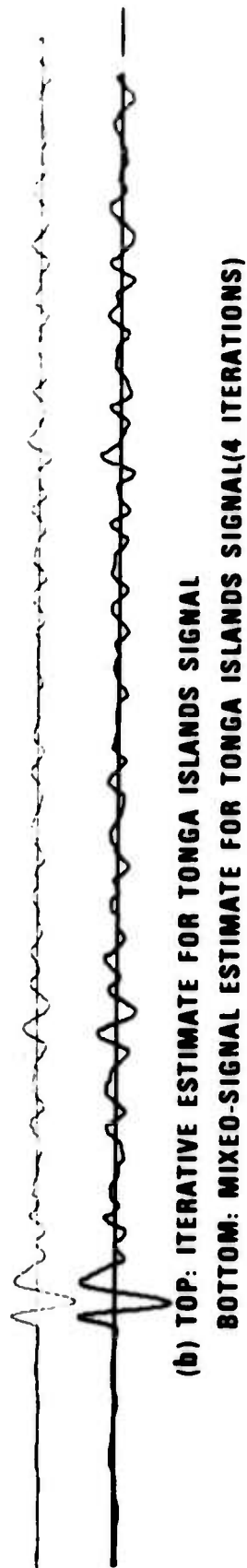


Figure 6. Comparison of the beam, mixed-signal and iterative-beam processors using the superimposed Tonga and Fox Islands signals (7 channels).

the results produced by the mixed-signal processor. Further, note the significant reduction in leakage signals* on these estimates over the results obtained using simple beam sums (Figures 6 a and c). For example, the leakage signal from the Tonga Islands event, which can be observed prior to the arrival of the Fox Islands signal in Figure 6c, is reduced by over 8 db in the estimates shown in Figure 6d.

The results from similar analyses of all 19 TFO channels shown in Figure 5 are shown in Figure 7. Again, the iterative-beam and mixed-signal processors yield practically identical results. Further, while the leakage signals in the 19-element beams (Figures 7a and c) are significantly reduced over those observed in the 7-element beams (Figure 6a and c), we note that the suppression of leakage signals using 19-elements and the simple beam is comparable to the attenuation obtained using the 7-element subarray and the iterative-beam or mixed-signal processor.

A further demonstration that the iterative approximation yields results identical to those produced by the mixed-signal processor is shown in Figure 8. Here, while only the signals from the Fox Islands event (Figure 3; 19 elements analyzed) are actually present, we sought estimates of signals from both the Fox and Tonga Islands. The "estimates" for the Tonga Islands

* The leakage signal is that proportion of Signal 1 which leaks into our estimate for Signal 2 (and vice versa).



(a) BEAM ON THE TONGA ISLANDS



(b) TOP: ITERATIVE ESTIMATE FOR TONGA ISLANDS SIGNAL
BOTTOM: MIXED-SIGNAL ESTIMATE FOR TONGA ISLANDS SIGNAL



(c) BEAM ON THE FOX ISLANDS



(d) TOP: ITERATIVE ESTIMATE FOR FOX ISLANDS SIGNAL(4 ITERATIONS)
BOTTOM: MIXED-SIGNAL ESTIMATE FOR FOX ISLANDS SIGNAL

5 sec

Figure 7. Comparison of the beam, mixed-signal and iterative-beam processors using the superimposed Tonga and Fox Islands signals (19 channels).

signal are, of course, leakage signals. As seen in Figures 8b and d, the estimates obtained using the iterative-beam and mixed-signal processors are virtually identical. Further, the simple beam estimate for the Fox Islands signal (Figure 8c) appears identical to the estimates obtained using the more sophisticated processors.

A more quantitative analysis of the leakage signals (Figures 8a and b) can be made by comparing the power in these signals. We justify this approach on the grounds that the leakage represents an additional noise signal which would appear in the estimate of the Tonga Islands signal, had one been present. Using a 35-second window beginning at a point corresponding to the first arrival of the Tonga Islands signal (Figures 8c and d), a measure of the power \bar{R} in the various estimates of the leakage signal is given as follows:

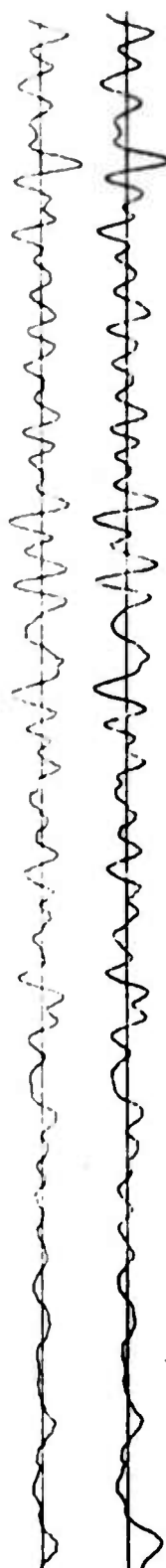
$$\bar{R} = [T^{-1} \sum_{t=1}^T \hat{s}^2(t) \Delta t]$$

where $\hat{s}(t)$ is the estimate for the leakage signal, and T is the length of the sample analyzed.

For the simple beam (Figure 8a), \bar{R} is $0.914\text{m}\mu^2$, while for the iterative-beam and mixed-signal estimates (Figure 8b), \bar{R} is found to be 0.174 and $0.176\text{m}\mu^2$, respectively. Thus, in this case, the more sophisticated processors yield an additional 7.2 db of coda attenuation over that provided by the simple beam. In



(a) BEAM ON THE TONGA ISLANDS



(b) TOP: ITERATIVE ESTIMATE FOR TONGA ISLANDS SIGNAL
BOTTOM: MIXED-SIGNAL ESTIMATE FOR TONGA ISLANDS SIGNAL(4 ITERATIONS)



(c) BEAM ON THE FOX ISLANDS



(d) TOP: ITERATIVE ESTIMATE FOR FOX ISLANDS SIGNAL
BOTTOM: MIXED-SIGNAL ESTIMATE FOR FOX ISLANDS SIGNAL(4 ITERATIONS)

← 5 sec →

Figure 8. Comparison of the beam, mixed-signal and iterative-beam processors using the Fox Islands signal (19 channels).

general, the coda attenuation capability of the mixed-signal processor (and its approximation, the iterative-beam processor) over that obtained using the simple beam is on the order of 3 to 5 db, although significantly more improvement can be expected if the signals are close in velocity space (Cohen, 1972).

Characteristics of the Iterative-Beam Processor

Having demonstrated that the iterative-beam processor yields solutions identical to those produced by the mixed-signal processor, we now examine some characteristics of the iterative approximation. Specifically, we discuss rate of convergence as a function of how the processor is applied, and the number of channels analyzed (i.e., the array size).

Two Signals - 7 Channels

Application of the iterative-beam processor to the superimposed Tonga and Fox Islands signals recorded on the seven inner elements of TFO (Figure 5, Channels 1-7) yields the results given in Table III and shown in Figures 9 through 12 (all signal estimates shown are normalized to the same peak amplitude). Figures 9a and 11a suggest that the two iterative processes are converging to the same answer, but that one, for which the initial beam is on the event of interest, is converging more quickly than the other. Even removing the predictable bias on the mid-iteration signal estimates (Figures 9b and 11b) does not completely correct

TABLE III
Iterative-Beam Analysis
Two-Signals 7-Channels

Signal 1 (Tonga Islands)
Initial Beam on Tonga Is.

Iteration	Maximum Amp. Sum Trace (mμ)
0	13.12
1	12.93
2	12.90
3	12.90
4	12.91

Signal 2 (Fox Islands)
Initial Beam on Fox Is.

Iteration	Maximum Amp. Sum Trace (mμ)
0	14.54
1	14.69
2	14.79
3	14.89
4	14.90

Initial Beam on Fox Is.

Iteration	Maximum Amp. Sum Trace (mμ)
1	9.48
2	11.31
3	12.00
4	12.33
5	12.52

Initial Beam on Tonga Is.

Iteration	Maximum Amp. Sum Trace (mμ)
1	11.35
2	13.61
3	14.32
4	14.62
5	14.73

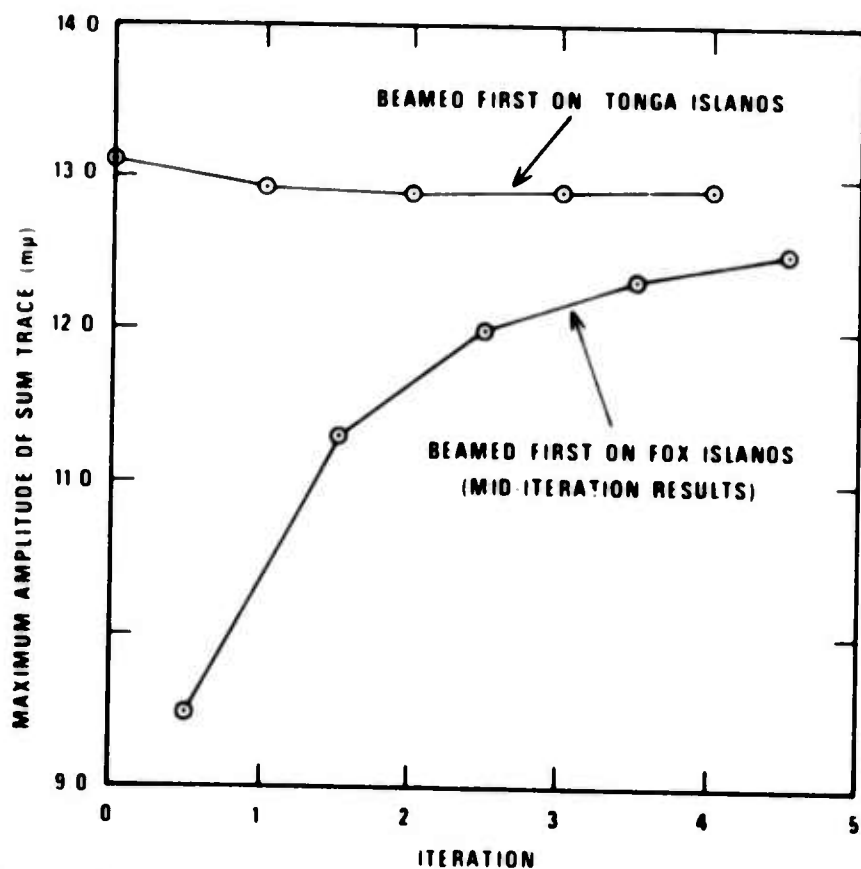


Figure 9a. Convergence characteristics for the Tonga Islands iterative-beam signal estimates, superimposed Tonga and Fox Islands signals, 7 channels.

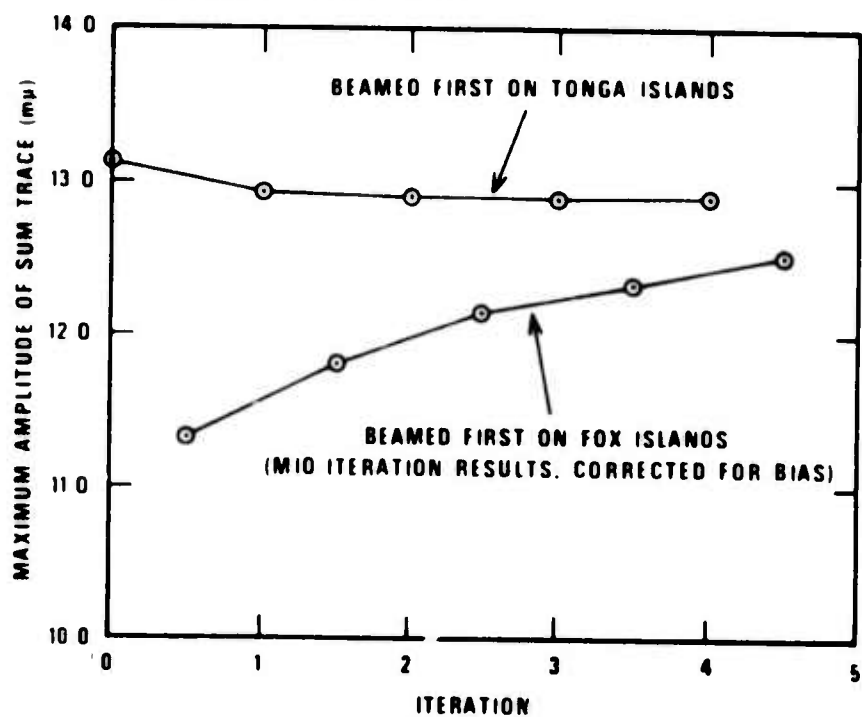
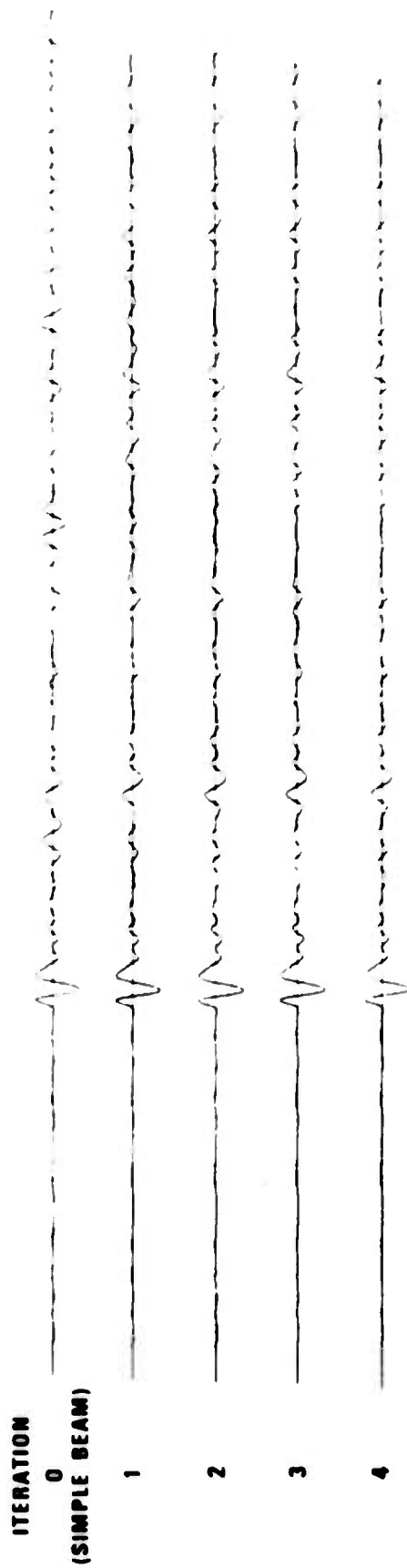
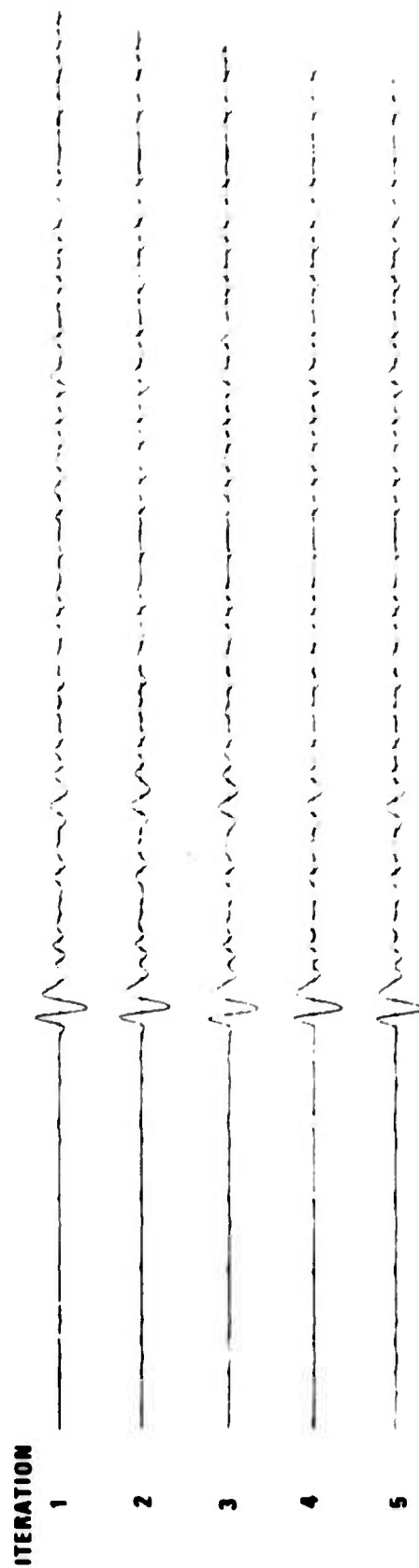


Figure 9b. Convergence characteristics for the Tonga Islands iterative-beam signal estimates, superimposed Tonga and Fox Islands signals, 7 channels, predictable bias removed.



(a) FIRST BEAM ON TONGA ISLANDS: RESULTS TAKEN AT END OF EACH ITERATION



(b) FIRST BEAM ON FOX ISLANDS: MID-ITERATION RESULTS

5 sec

Figure 10. Iterative-beam Tonga Islands signal estimates, superimposed Tonga and Fox Islands signals, 7 channels

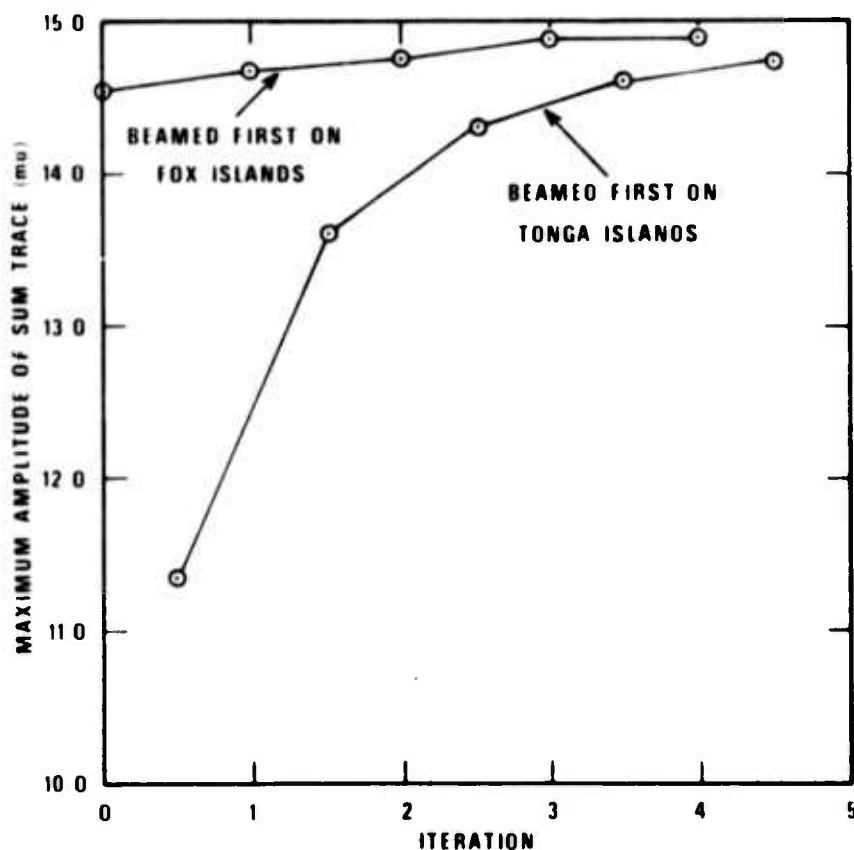


Figure 11a. Convergence characteristics for the Fox Islands iterative-beam signal estimates, superimposed Tonga and Fox Islands signals, 7 channels.

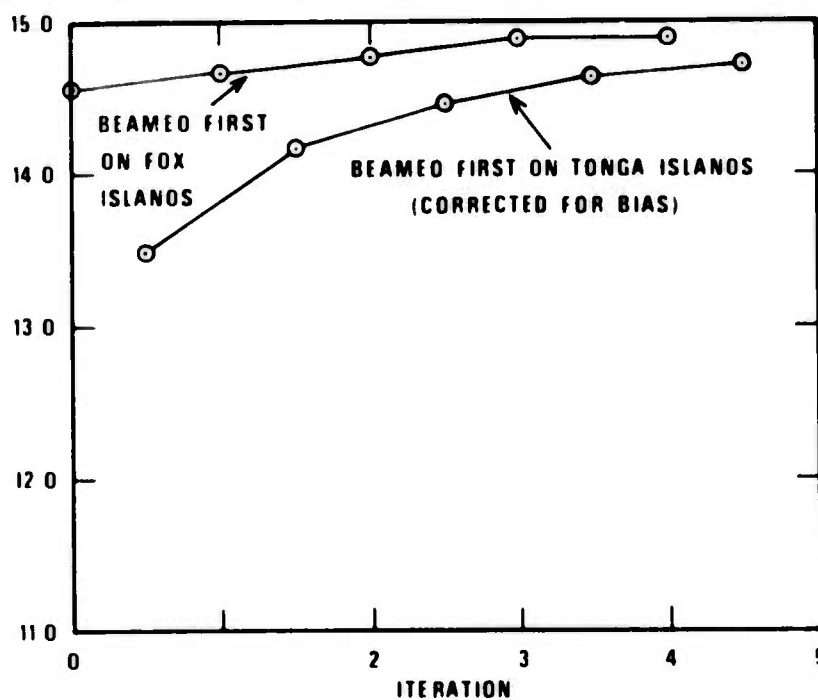
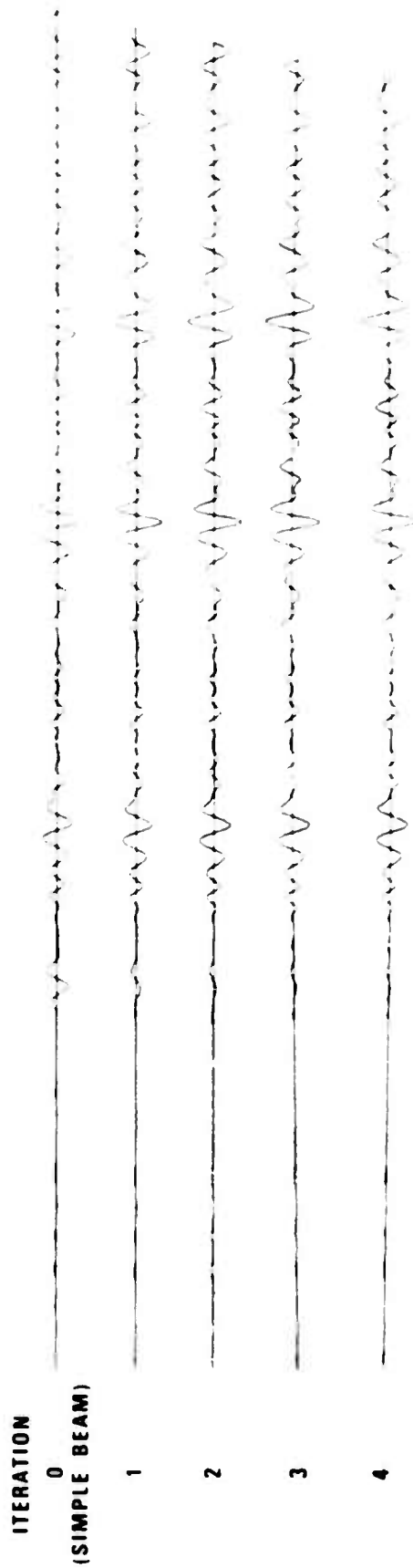
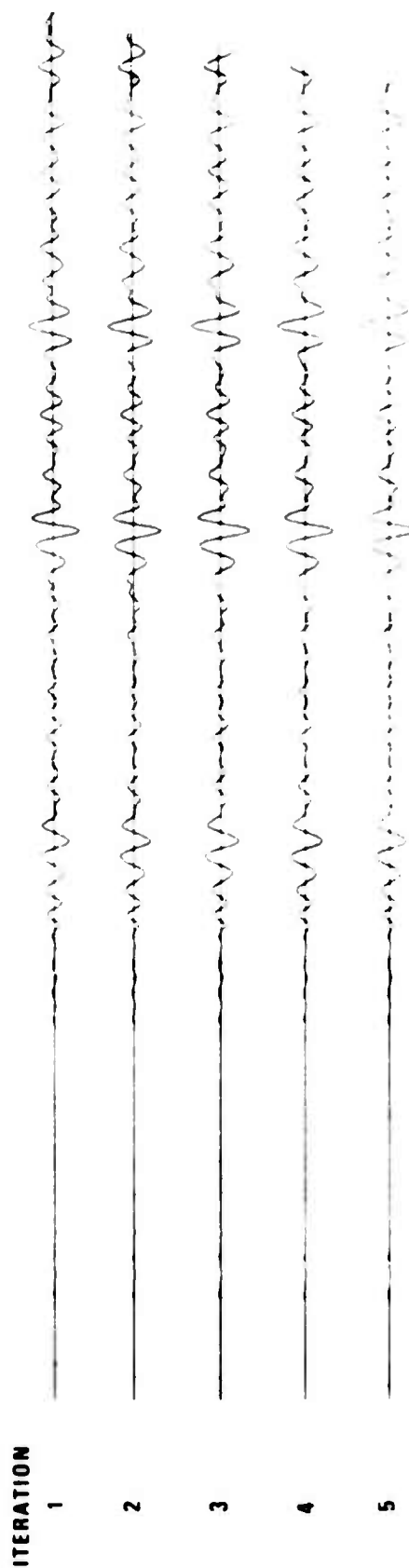


Figure 11b. Convergence characteristics for the Fox Islands iterative-beam signal estimates, Tonga and Fox Islands signals, predictable bias removed.



(a) FIRST BEAM ON FOX ISLANDS: RESULTS TAKEN AT END OF EACH ITERATION



(b) FIRST BEAM ON TONGA ISLANDS: MID-ITERATION RESULTS

← 5 sec →

Figure 12. Iterative-beam Fox Islands signal estimates, superimposed Tonga and Fox Islands signals, 7 channels.

for the contamination of a given signal by its own echoes. Further, as seen in Figure 10b, the mid-iteration signal estimates for the Tonga Islands event (initial beam on the Fox Islands) exhibit precursors to the first arrival which derive from echoes of the Tonga Islands signal. It should be noted that the large precursors on the signal estimation for the Fox Islands event (Figure 12a) derive from leakage of the Tonga Islands signal, and not from echoes of the Fox Islands event (though these must be present).

The results obtained here amplify our earlier comments on the proper mode for implementation of the iterative-beam processor. That is, one should beam initially on the signal of interest, and use only those signal estimates produced at the end of a complete iteration.

Choice of a test for convergence of the iterative process is somewhat subjective. For many qualitative purposes (e.g. detections), the first iteration is significantly improved over the beam to such an extent that the process can be terminated without a test. In general, however, a quantitative decision has to be made as to what constitutes a "significant improvement". Though the analyses discussed in this report were arbitrarily terminated on the 4th or 5th iteration, we could have, for example, computed the rms amplitude of the difference between successive signal estimates, and terminated the process when the rms value fell below a prescribed level.

For the 7-channel, iterative-beam computations discussed here, the total CPU time for the Tonga and Fox Island signal estimates (four iterations each) on an IBM 360/44 was on the order of 13 minutes. For both signals and only one iteration on each solution, the time is approximately 3.0 minutes. This is one-half the CPU time required for the corresponding solutions using the mixed-signal processor (~6 minutes). One must also remember that for more than 7 elements, the iterative process will converge even more accurately in two iterations for any number of channels, while the number of convolutions needed per point for the maximum likelihood approach increases in proportion to N , the number of channels. As a result, the maximum-likelihood processor is impractical for LASA short-period data, while iterative beamforming is practical.

Two Signals - 19 Channels

For the superimposed Tonga and Fox Islands signals recorded on a 19-element TFO array (Figure 5), the iterative-beam processor yields the results given in Table IV and shown in Figures 13 through 16.

The total CPU time for the signal estimates (four iterations on each signal) was on the order of 30 minutes. However, because the iterative process converged so rapidly for the 19-channel cases, the CPU time actually required to separate the signals - that is, the time required for one iteration on each signal - is estimated

TABLE IV
Iterative-Beam Analysis
Two-Signal 19-Channels

Signal 1 (Tonga Islands)
Initial Beam on Tonga Is.

Iteration	Maximum Amp. Sum Trace (mμ)
0	12.18
1	12.48
2	12.53
3	12.54
4	12.53

Signal 2 (Fox Islands)
Initial Beam on Fox Is.

Iteration	Maximum Amp. Sum Trace (mμ)
0	14.21
1	14.50
2	14.50
3	14.52
4	14.52

Initial Beam on Fox Is.

Iteration	Maximum Amp. Sum Trace (mμ)
1	11.30
2	12.18
3	12.38
4	12.44
5	12.47

Initial Beam on Tonga Is.

Iteration	Maximum Amp. Sum Trace (mμ)
1	13.59
2	14.35
3	14.52
4	14.56
5	14.56

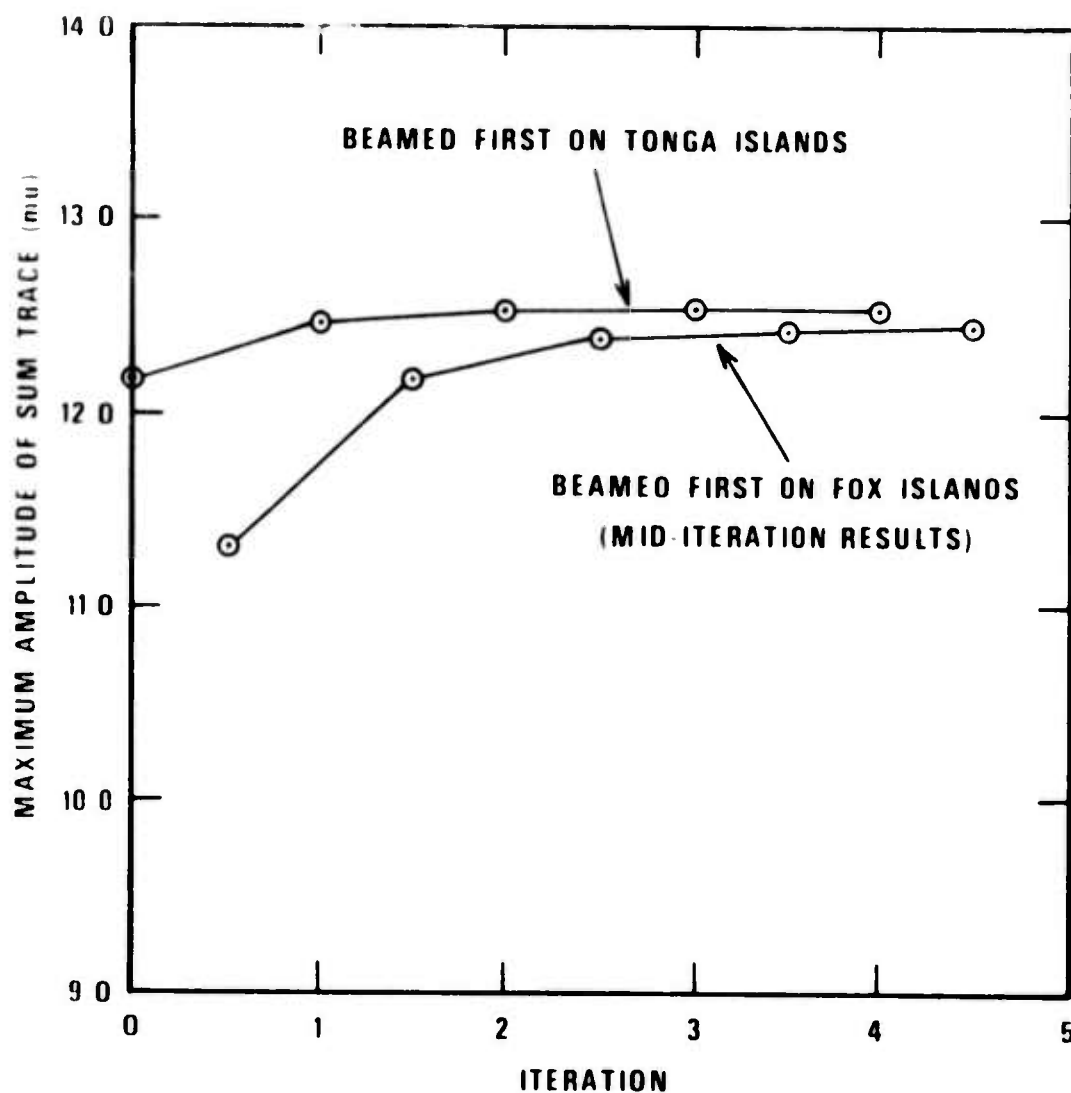
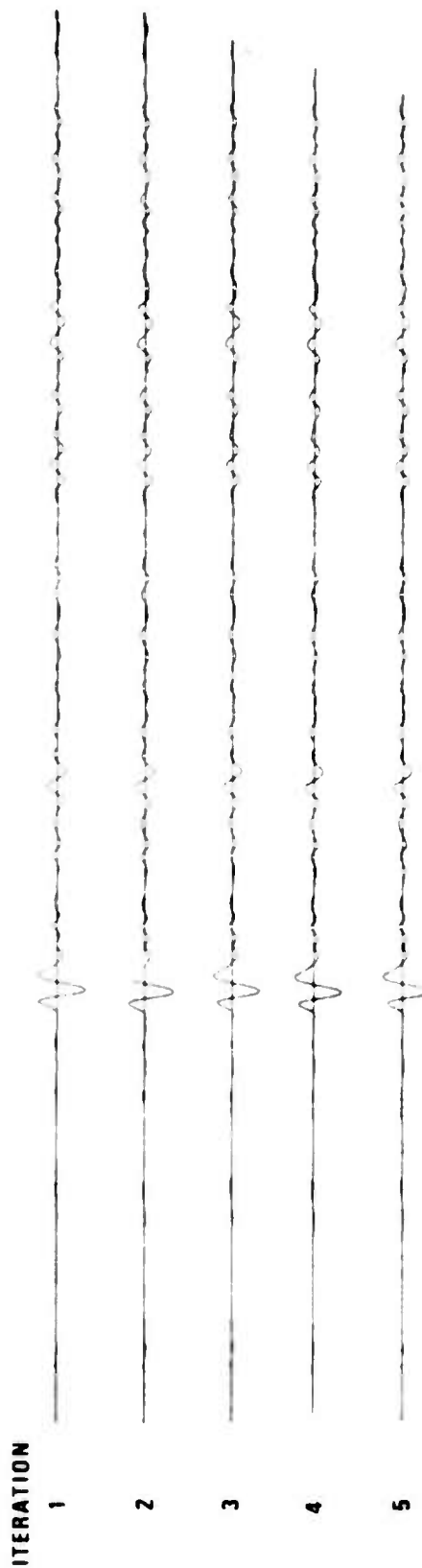


Figure 13. Convergence characteristics for the Tonga Islands iterative-beam signal estimates, superimposed Tonga and Fox Islands signals, 19 channels.



(a) FIRST BEAM ON TONGA ISLANDS. RESULTS TAKEN AT END OF EACH ITERATION



(b) FIRST BEAM ON TONGA ISLANDS. MID-ITERATION RESULTS

5 sec

Figure 14. Iterative-beam Tonga Islands signal estimates, superimposed Tonga and Fox Islands signals, 19 channels.

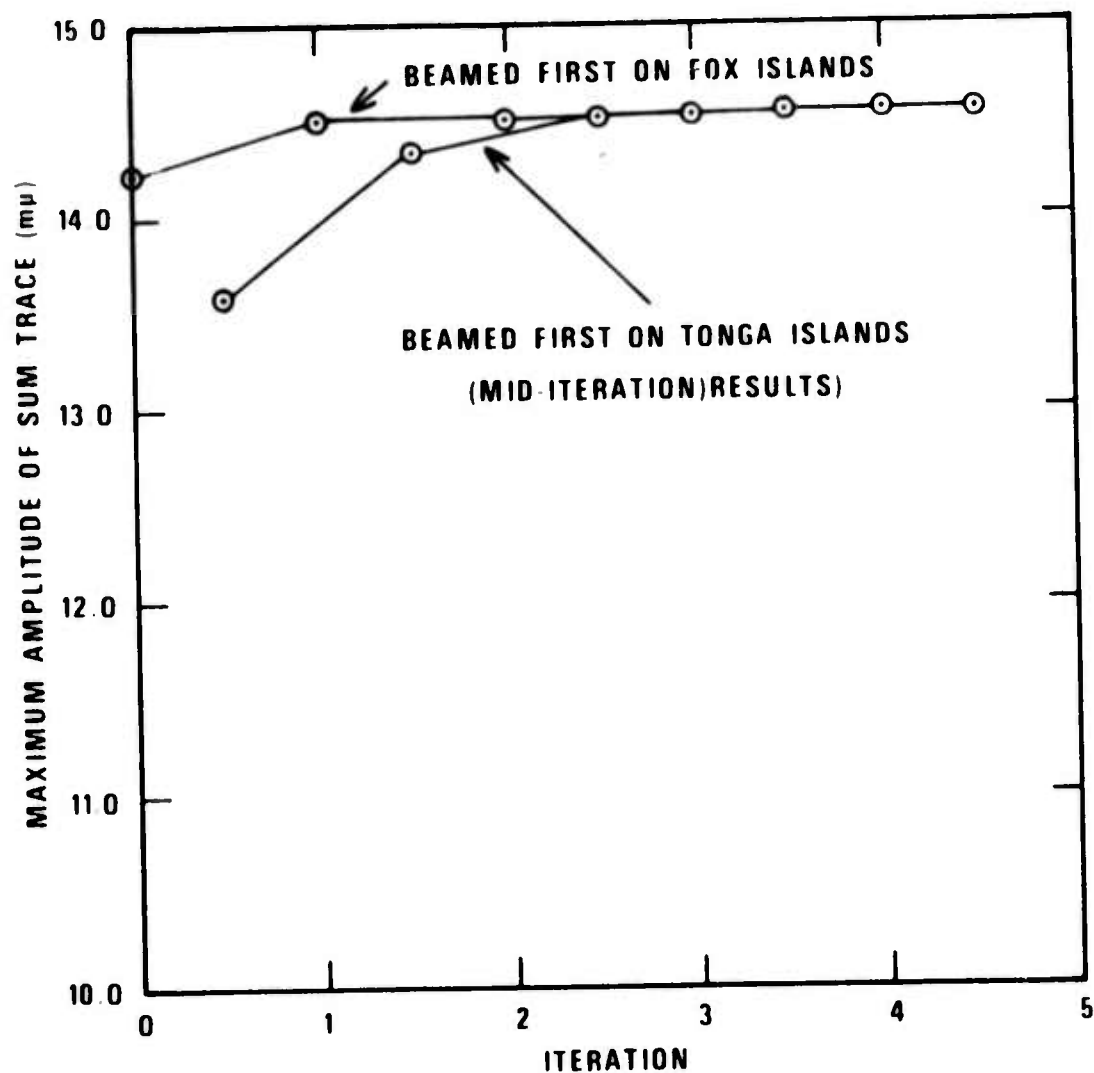
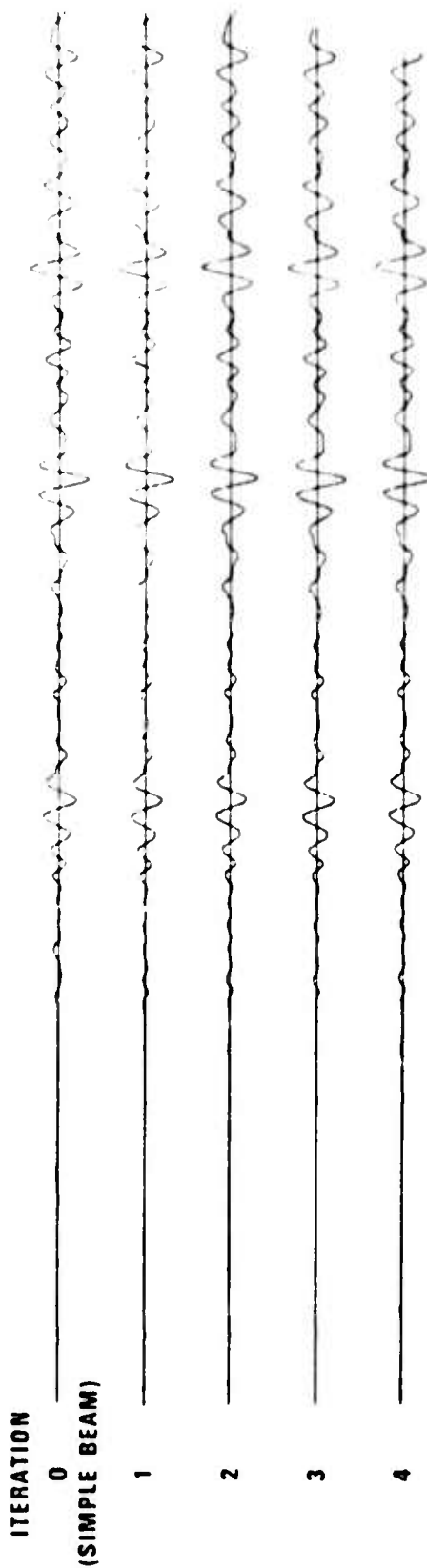
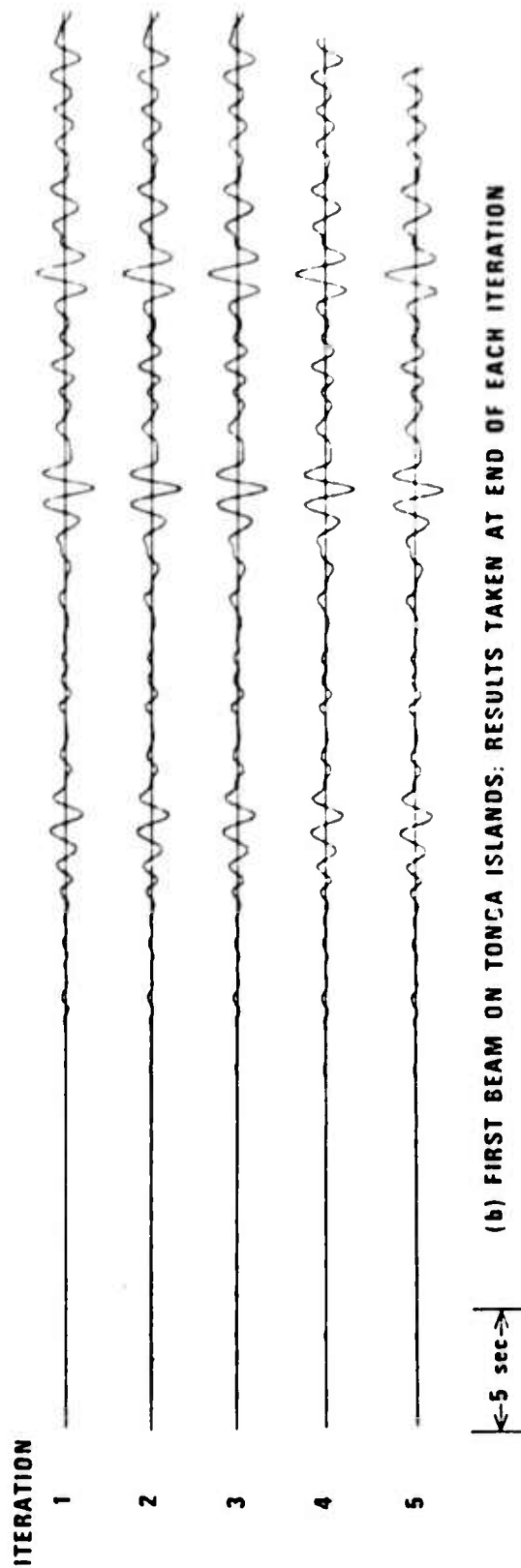


Figure 15. Convergence characteristics for the Fox Islands iterative-beam signal estimates, superimposed Tonga and Fox Islands signals, 19 channels.



(a) FIRST BEAM ON FOX ISLANDS: RESULTS TAKEN AT END OF EACH ITERATION



(b) FIRST BEAM ON TONCA ISLANDS: RESULTS TAKEN AT END OF EACH ITERATION

Figure 16. Iterative-beam Fox Islands signal estimates, factors, superimposed Tonga and Fox Islands signals, 19 channels.

at 7 minutes. This compares favorably with the CPU time required for corresponding solutions using the mixed-signal processor (~12 minutes for 19 channels).

One Signal - 7 Channels

Table V and Figures 17 through 20 show the results of processing the Fox Islands signal (Figure 3) under the assumption that two signals - one from the Fox Islands and one from the Tonga Islands - are present. A plot of the sum trace rms amplitude for the non-existent Tonga Islands signal is shown in Figure 17 as a measure of the portion of the Fox Island events which would leak into our estimates of the Tonga Islands signal (had a Tonga Island signal been present).

In this case, beaming first on the Fox Islands and extracting the Tonga Islands signal (noise) estimates at mid-iteration yields solutions for the Tonga Islands event which stabilize more quickly than those produced by bearing first on this non-existent event. This is not surprising when one considers that the estimates for the non-existent Tonga Islands event which are stripped out when one beams first on this event consist of a combination of noise and leakage from the Fox Islands event. By beaming first on the Fox Islands event and stripping out its signal, leakage into the Tonga Islands estimate is minimized in the early iterations.

These data suggest that if it is not known whether a second signal is present, or under low signal-to-noise

TABLE V
Iterative-Beam Analysis
One-Signal 7-Channels

Signal 1 (Tonga Islands)
Initial Beam on Tonga Is.

Iteration	Sum Trace rms (mμ)
0	2.311
1	1.108
2	0.782
3	0.697
4	0.676

Signal 2 (Fox Islands)
Initial Beam on Fox Is.

Iteration	Maximum Amp. Sum Trace (mμ)
0	15.34
1	15.20
2	15.17
3	15.15
4	15.19

Initial Beam on Fox Is.

Iteration	Sum Trace rum (mμ)
1	0.494
2	0.591
3	0.628
4	0.646
5	0.657

Initial Beam on Tonga Is.

Iteration	Maximum Amp. Sum Trace (mμ)
1	11.94
2	14.16
3	14.77
4	14.96
5	15.06

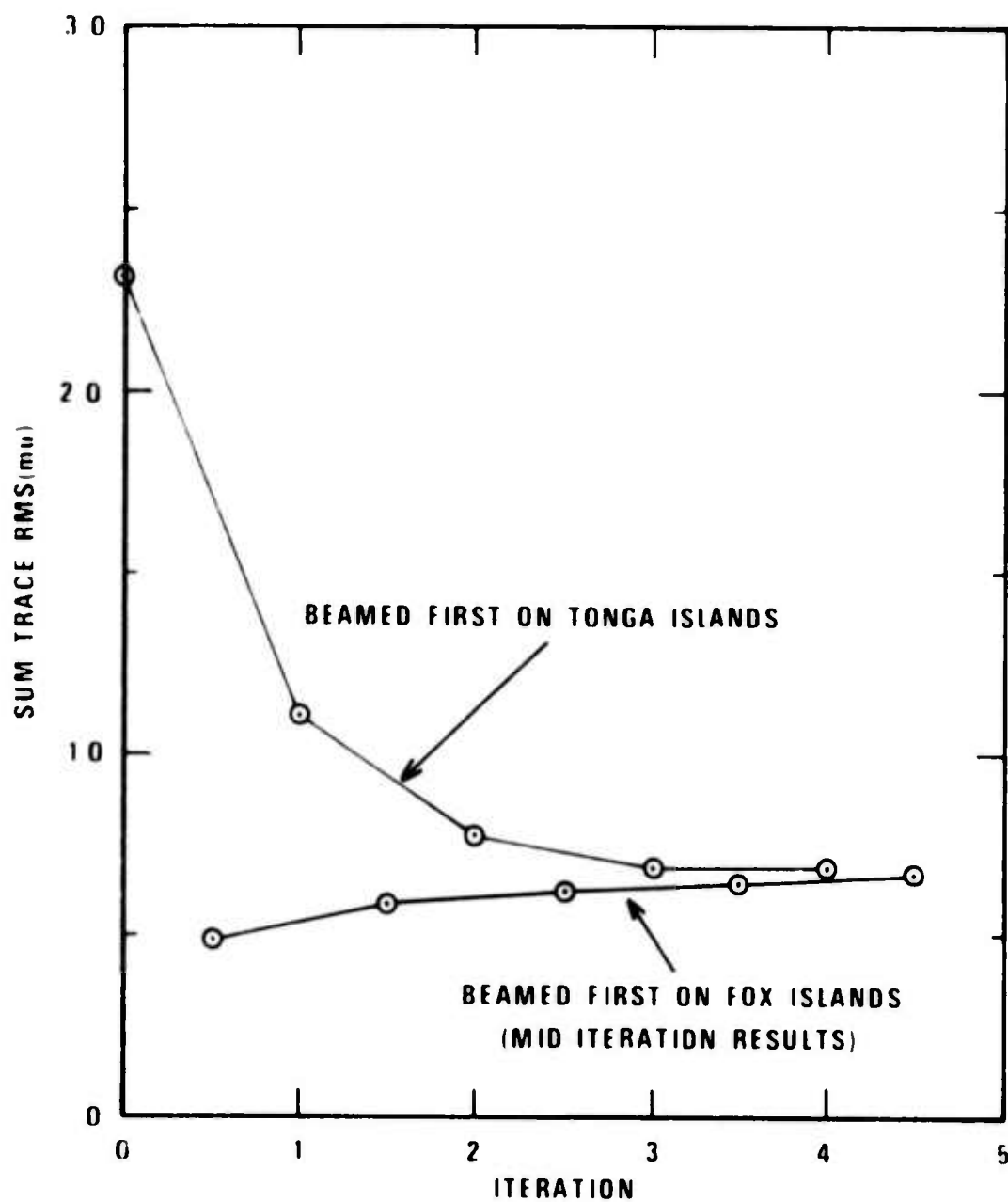
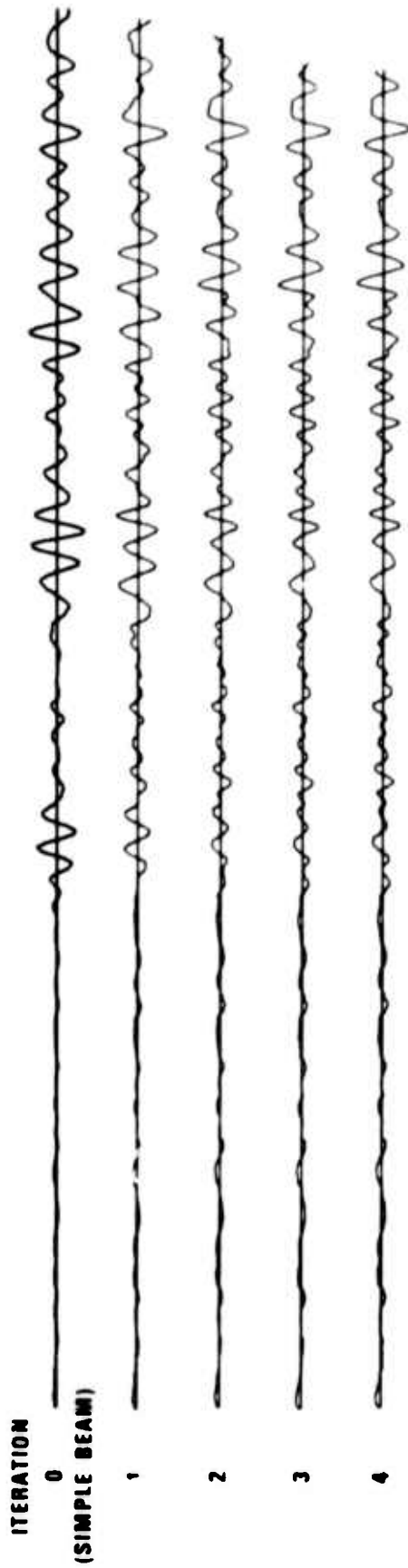
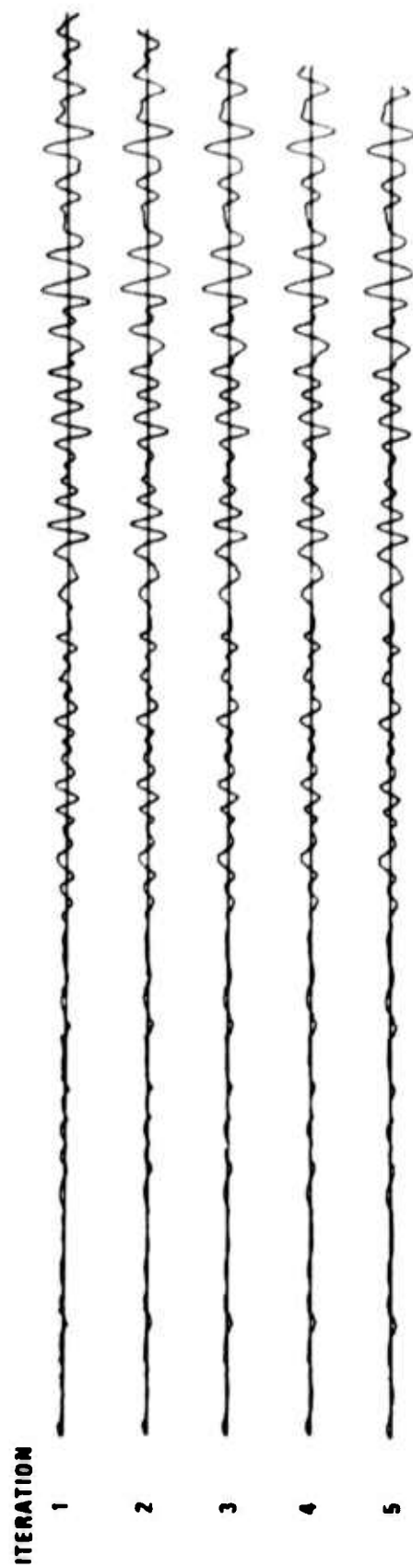


Figure 17. Convergence characteristics for the Tonga Islands iterative-beam signal estimates, Fox Islands signal, 7 channels.



(a) FIRST BEAM ON TONGA ISLANDS; RESULTS TAKEN AT END OF EACH ITERATION



(b) FIRST BEAM ON FOX ISLANDS; MID-ITERATION RESULTS

← 5 sec →

Figure 18. Iterative-beam Tonga Islands signal estimates, Fox Islands signal, 7 channels.

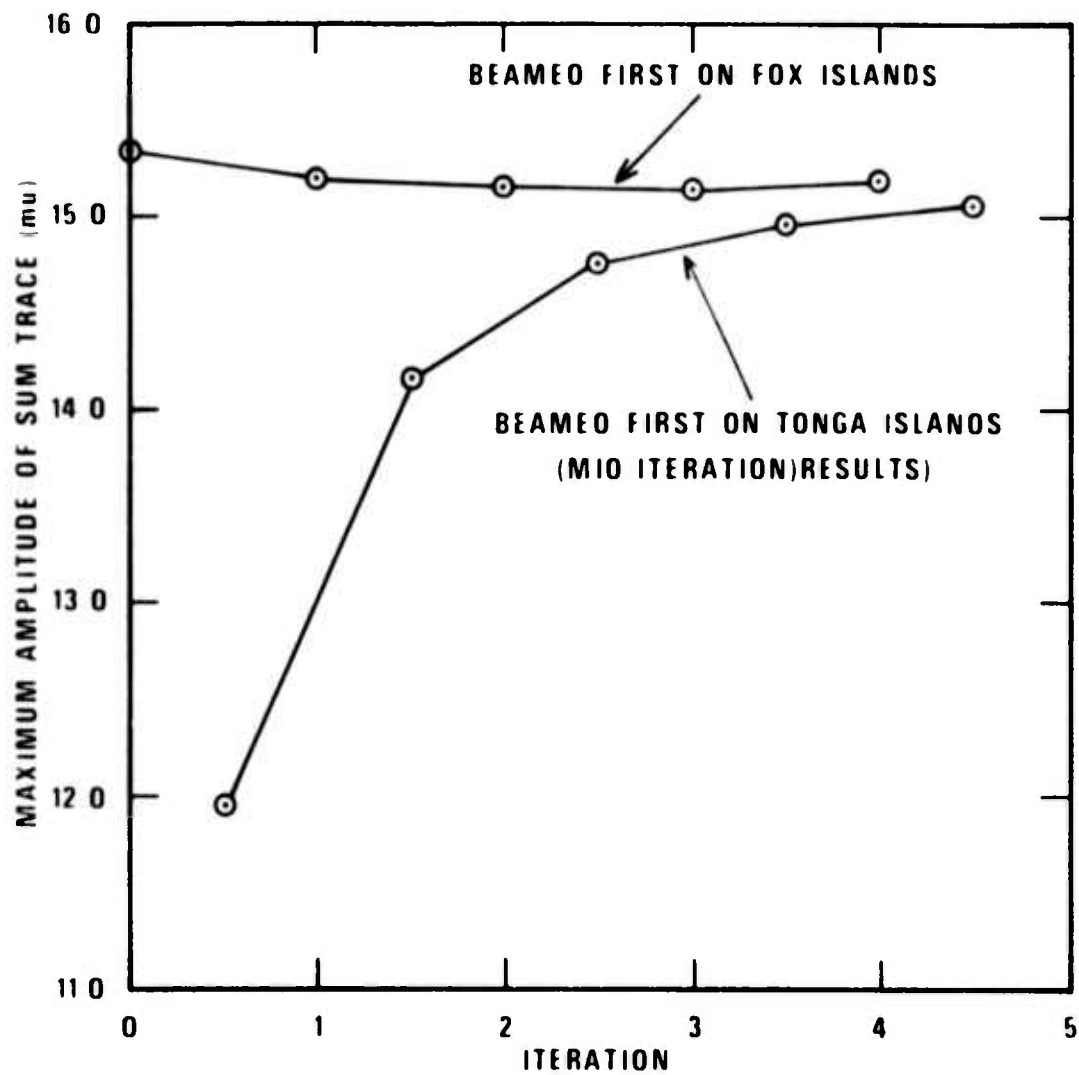


Figure 19. Convergence characteristics for the Fox Islands iterative-beam signal estimates, Fox Islands signal, 7 channels.

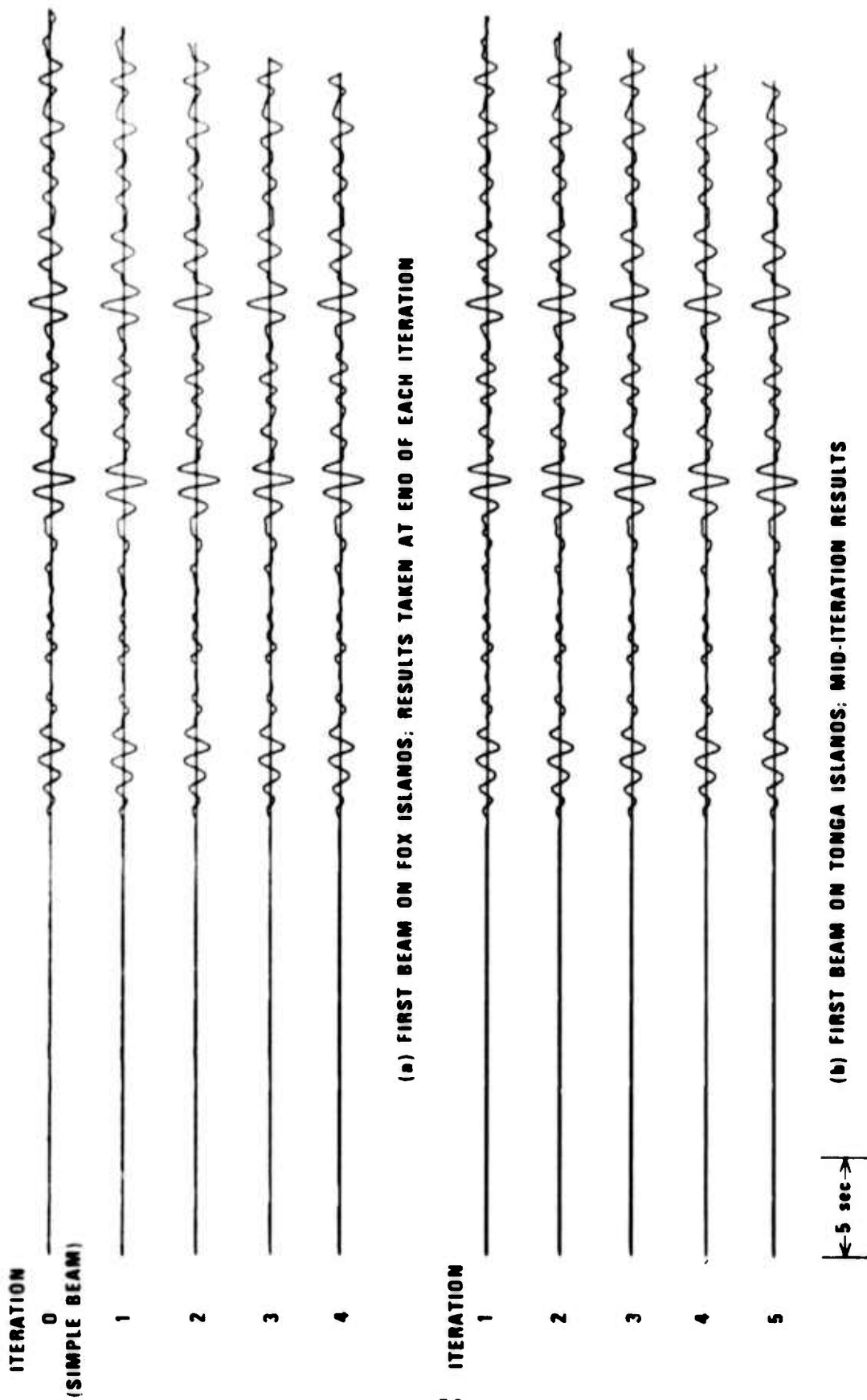


Figure 20. Iterative-beam Fox Islands signal estimates, Fox Islands signal, 7 channels.

conditions for the second event (second events signal buried in the coda of a large event), one should beam first on the known event's epicenter, and examine the mid-iteration signal estimates for the second event. If a weak, second event is indeed present, its signal estimate will be biased, but its waveform will stabilize more rapidly than if we beam first on this signal.

Thus, when the mere existence of a weak second signal, rather than its amplitude and detailed waveform, is of interest, it would seem best to initially beam on the first signal.

One Signal - 19 Channels

Application of the iterative-beam processor of the Fox Islands signal recorded on a 19-element TFO array (Figure 3) yields the results shown in Table VI and Figures 21 through 24. Except for a scale factor, the various signal estimates for the Fox Islands event are almost indistinguishable from one another. Due to the large number of array elements (and hence, in this case, the large aperture of the array) signal estimates for the non-existent Tonga Islands event stabilized after one iteration. If a weak Tonga Islands signal had been present, however, it would be best for detection purposes to extract the mid-iteration signal estimates for this event produced by beaming first on the Fox Islands event.

TABLE VI
Iterative-Beam Analysis
One-Signal 19-Channels

Signal 1 (Tonga Islands)
Initial Beam on Tonga Is.

Iteration	Sum Trace rms (mμ)
0	0.956
1	0.447
2	0.423
3	0.421
4	0.421

Signal 2 (Fox Islands)
Initial Beam on Fox Is.

Iteration	Maximum Amp. Sum Trace (mμ)
0	14.27
1	14.29
2	14.30
3	14.29
4	14.26

Initial Beam on Fox Is.

Iteration	Sum Trace rms (mμ)
1	0.385
2	0.405
3	0.412
4	0.415
5	0.418

Initial Beam on Tonga Is.

Iteration	Maximum Amp. Sum Trace (mμ)
1	13.81
2	14.11
3	14.18
4	14.21
5	14.24

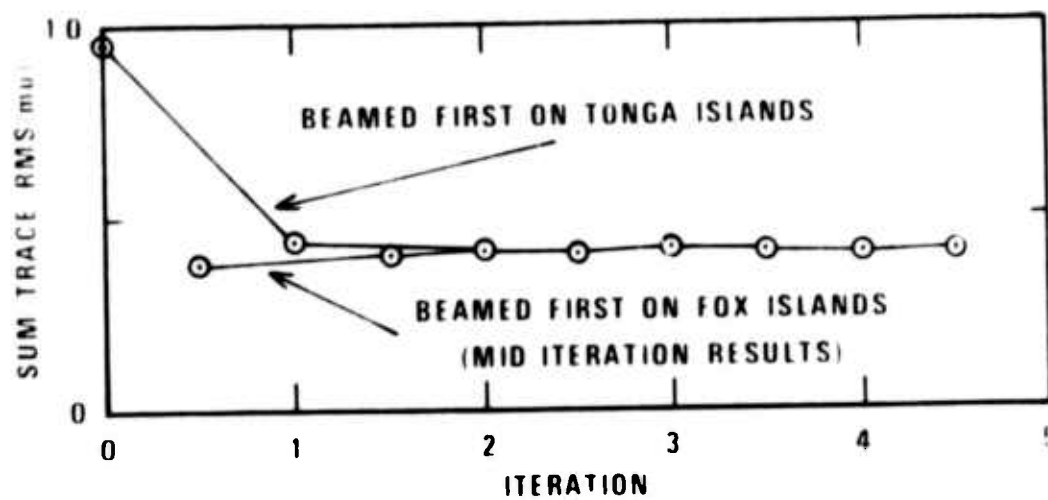


Figure 21. Convergence characteristics for the Tonga Islands iterative-beam signal estimates, Fox Islands signal, 19 channels.

ITERATION

0



1



2



3



4



(a) FIRST BEAM ON TONGA ISLANDS: RESULTS TAKEN AT END OF EACH ITERATION

ITERATION

1



2



3



4



5



5 sec

(b) FIRST BEAM ON FOX ISLANDS: MID-ITERATION RESULTS

Figure 22. Iterative-beam Tonga Islands signal estimates, Fox Islands signal, 19 channels.

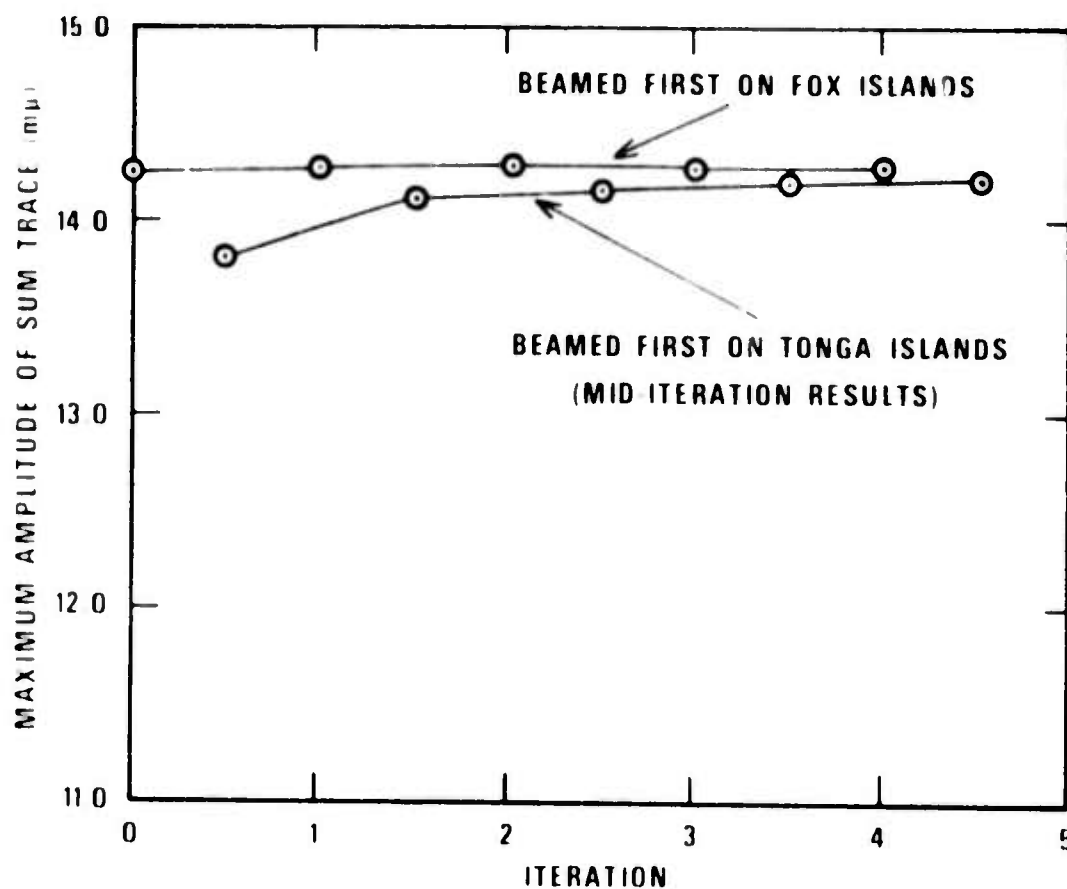


Figure 23. Convergence characteristics for the Fox Islands iterative-beam signal estimates, Fox Islands signal, 19 channels

ITERATION

0

1

2

3

4

(a) FIRST 4M ON FOX ISLANDS: RESULTS TAKEN AT END OF EACH ITERATION

ITERATION

1

2

3

4

5

← 5 sec →

(b) FIRST BEAM ON TONGA ISLANDS: MID-ITERATION RESULTS

Figure 24. Iterative-beam Fox Islands signal estimates, Fox Islands signal, 19 channels.

Noise

Let us now examine the signal estimates obtained using the beam, iterative-beam, and mixed-signal processors in cases where only noise is present. The first noise sample analyzed was recorded prior to the arrival of the Fox Islands signal. Application of the processors to the noise recorded on 7 and 19 channels yields the results listed in Tables VII a and b, and shown in Figures 25 and 26, respectively. In every case, the signal estimates produced on the fourth iteration, regardless of the event beamed initially, were identical. The noise waveforms converge as quickly as the signal waveforms that would be expected from the linearity of the process.

Analyses of the noise recorded prior to the arrival of the Tonga Islands signal yield similar results. For that reason, only the tabulated values for the beam and iterative-beam computations are given here (Tables VIII a and b).

Of primary concern to us is a comparison of the rms levels for the beam and iterative-beam noise estimates. We might expect the iterative-beam processor to be similar to the simple beam when processing noise; that is, we expect both processors to reduce the rms levels of the final noise estimates by something on the order of the $N^{1/2}$, where N is the number of channels processed.

Table IX shows a comparison of the rms levels for

TABLE VIIa
 Iterative-Beam Analysis
 Noise (Fox Islands) 7-Channels

Signal 1 (Tonga Islands)
 Initial Beam on Tonga Is.

Iteration	Sum Trace rms (mμ)
0	0.282
1	0.250
2	0.236
3	0.230
4	0.229

Signal 2 (Fox Islands)
 Initial Beam on Fox Is.

Iteration	Sum Trace rms (mμ)
0	0.290
1	0.274
2	0.273
3	0.274
4	0.277

Initial Beam on Fox Is.

Iteration	Sum Trace rms (mμ)
1	0.101
2	0.144
3	0.170
4	0.186
5	0.198

Initial Beam on Tonga Is.

Iteration	Sum Trace rms (mμ)
1	0.103
2	0.149
3	0.181
4	0.206
5	0.225

TABLE VIIb
 Iterative-Beam Analysis
 Noise (Fox Islands) 19-Channels

Signal 1 (Tonga Islands)
 Initial Beam on Tonga Is.

Iteration	Sum Trace rms (mμ)
0	0.187
1	0.158
2	0.150
3	0.147
4	0.147

Signal 2 (Fox Islands)
 Initial Beam on Fox Is.

Iteration	Sum Trace rms (mμ)
0	0.204
1	0.192
2	0.189
3	0.188
4	0.187

Initial Beam on Fox Is.

Iteration	Sum Trace rms (mμ)
1	0.101
2	0.121
3	0.129
4	0.134
5	0.138

Initial Beam on Tonga Is.

Iteration	Sum Trace rms (mμ)
1	0.116
2	0.150
3	0.166
4	0.174
5	0.179

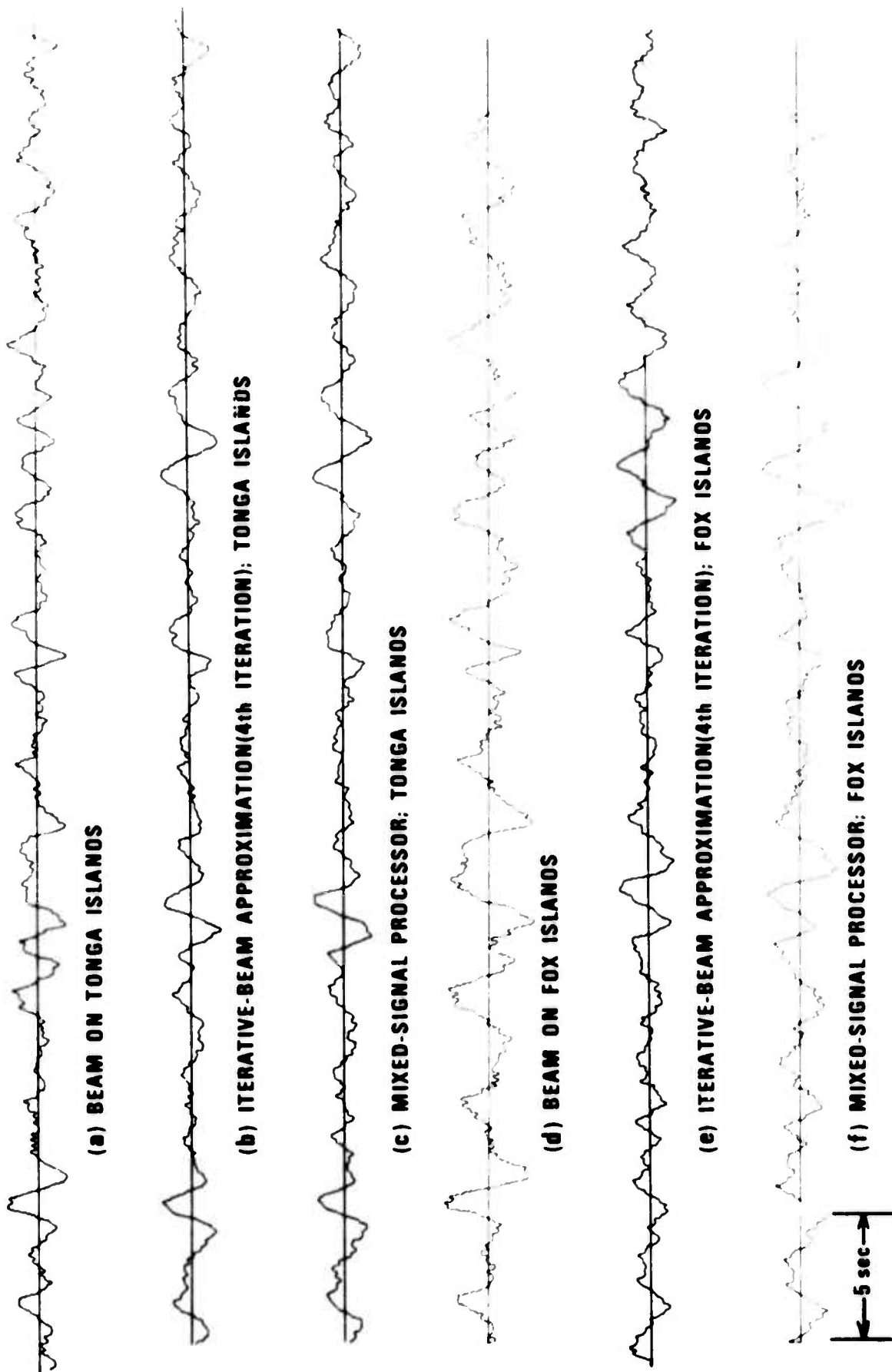


Figure 25. Comparison of noise estimates from noise recorded prior to the arrival of the Fox Islands signal, 7 channels.

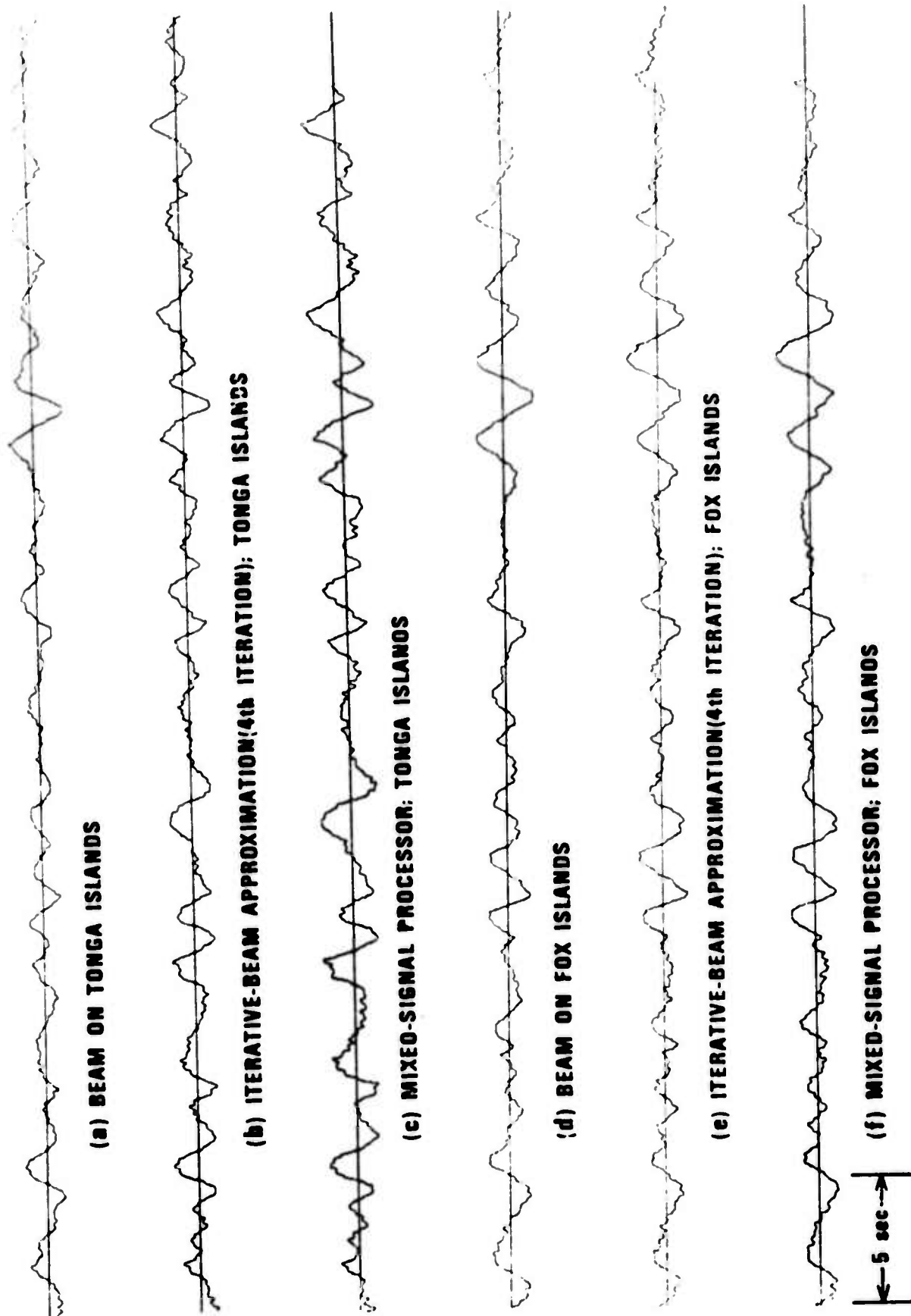


Figure 26. Comparison of noise estimates from noise recorded prior to the arrival of the Fox Islands signal, 19 channels.

TABLE VIIIa
Iterative-Beam Analysis
Noise (Tonga Islands) 7-Channels

Signal 1 (Tonga Islands)
Initial Beam on Tonga Is.

Iteration	Sum Trace rms (μ)
0	0.216
1	0.220
2	0.227
3	0.232
4	0.237

Signal 2 (Fox Islands)
Initial Beam on Fox Is.

Iteration	Sum Trace rms (μ)
0	0.182
1	0.157
2	0.154
3	0.157
4	0.162

Initial Beam on Fox Is.

Iteration	Sum Trace rms (μ)
1	0.115
2	0.161
3	0.188
4	0.205
5	0.218

Initial Beam on Tonga Is.

Iteration	Sum Trace rms (μ)
1	0.078
2	0.106
3	0.124
4	0.137
5	0.146

TABLE VIIIb
Iterative-Beam Analysis
Noise (Tonga Islands) 19-Channels

Signal 1 (Tonga Islands)
Initial Beam on Tonga Is.

Iteration	Sum Trace rms (mμ)
0	0.143
1	0.151
2	0.158
3	0.162
4	0.165

Signal 2 (Fox Islands)
Initial Beam on Fox Is.

Iteration	Sum Trace rms (mμ)
0	0.102
1	0.091
2	0.097
3	0.102
4	0.105

Initial Beam on Fox Is.

Iteration	Sum Trace rms (mμ)
1	0.109
2	0.139
3	0.153
4	0.159
5	0.163

Initial Beam on Tonga Is.

Iteration	Sum Trace rms (mμ)
1	0.071
2	0.088
3	0.097
4	0.102
5	0.105

TABLE IX

Comparison of rms Noise Estimates
Two-Sided F-Test ($\alpha=.10$)

Identification of Noise Traces	No. Chan.	Beamed Region	s1 Beam rms (mμ)	s2 Iterative- Beam* rms (mμ)	$\frac{s_1^2}{\delta_2^2}$	$\frac{s_2^2}{\delta_1^2}$	F .05,60,60
Fox Is. Event	7	Tonga Is.	.282	.229	1.51		1.53
	7	Fox Is.	.290	.277	1.10		
	19	Tonga Is.	.187	.147	1.57		
	19	Fox Is.	.204	.187	1.19		
Tonga Is. Event	7	Tonga Is.	.216	.237		1.20	
	7	Fox Is.	.182	.162	1.26		
	19	Tonga Is.	.143	.165		1.33	
	19	Fox Is.	.102	.105		1.06	

* 8'th iteration

the noise estimates produced by the beam and iterative-beam processors. To test the significance of the differences observed, we use a two sided F-test. The degrees of freedom for the noise estimates is given as follows:

$$\text{degrees of freedom} = 2BT$$

where B is the bandwidth of the noise, and T is the sample length. For $B \sim 1$ Hz, and a sample length of 35 seconds, $2BT \approx 70$. If we take a nominal value of 60 for the degrees of freedom, recourse to the standard tables for $F(05, v_1, v_2)$ yields a value of 1.53 for the two-sided F-test with $\alpha = 0.10$. Only one value for the rms ratios, that of the 19 channel Tonga Islands noise estimate computed using noise recorded prior to the Fox Islands event, exceeds this value (1.57 versus 1.53); the significance of the difference in the rms noise values for this case may be due to coherent noise propagating across the array from the direction of the Tonga Islands region. However, for $\alpha = 0.10$, we would expect 1 out of 10 ratio values to exceed the F-test value. Thus the data of Table IX indicate that the rms values for the beam and iterative-beam noise estimates are not significantly different. Further, as the 19-element TFO array, and possibly the 7-element array as well, can be expected to reduce the rms noise level on the beamed trace by a factor of $N^{1/2}$ over the rms noise level on the individual channels, so too, apparently, does the iterative beam (and,

hence, the mixed-signal processor) reduce the rms level of the noise estimates by the $N^{\frac{1}{2}}$. However, theoretical considerations suggest that this may not be true if the two signals are close together in velocity space.

CONCLUSIONS

In the limit, the iterative-beam processor converges to the mixed-signal processor. Further, the iterative-beam processor has great practical (and intuitive) appeal. For seven or more array elements, the iterative process converges in a few iterations, requiring only a few shift and sum operations per data point, while the mixed-signal (maximum likelihood) processor requires a convolution for every data point.

For many qualitative purposes, one iteration yields satisfactory convergence.

When two signals are present, each having approximately the same amplitude, one should beam first on the signal of interest, and use only those signal estimates produced at the end of a complete iteration. If one signal is considerably stronger than the other, however, the initial beam should be on the event corresponding to the larger signal, and the estimate for the smaller signal, although biased, extracted at mid-iteration.

The data suggest that the iterative-beam processor (and hence, the mixed-signal processor) reduces the rms noise level for traces well separated in velocity space by the $N^{1/2}$, where N is the number of channels.

ACKNOWLEDGEMENTS

The authors gratefully acknowledge the assistance of Mr. John W. Lambert for his programming of the iterative-beam processor. Mr. Travis J. Dutterer assisted in performing the computations related to the mixed-signal processor.

REFERENCES

- Cohen, T. J., 1972, Coda suppression capabilities of the beam and mixed-signal processor: Seismic Data Laboratory Report No. 298, Teledyne Geotech, Alexandria, Virginia.
- Dean, W. C., Shumway, R. H. and Duris, C. S., 1968, Best linear unbiased estimation for multivariate stationary processes: Seismic Data Laboratory Report No. 207, Teledyne Geotech, Alexandria, Virginia.
- Passechnik, I. P., 1972, Some possibilities of interpretation of array stations data, in: Proceedings from the seminar on seismology and seismic arrays, Royal Norwegian Council for Scientific and Industrial Research, Editors: E. S. Husebye and H. Bungum.
- Shumway, R. H., 1972, Some applications of a mixed signal processor: Seismic Data Laboratory Report No. 280, Teledyne Geotech, Alexandria, Virginia.
- Smart, E., 1972, FKCOMB, A fast general-purpose array processor: Seismic Array Analysis Center Report No. 9, Teledyne Geotech, Alexandria, Virginia.

APPENDIX I

Theoretical Proof of the Equivalence of Iterative
Two-Signal Beaming and Maximum-Likelihood Processing

The Fourier Transform of the data on the k 'th channel is given by

$$Y_k(\omega) = S_1(\omega) e^{-j\omega T_{k1}} + S_2(\omega) e^{-j\omega T_{k2}} + N_k(\omega), \quad (A-1)$$

where $j = \sqrt{-1}$.

Then the first estimate of S_1 , given $\{Y_k(\omega)\}_{k=1}^N$, is:

$$\begin{aligned} \hat{S}_1^{(1)}(\omega) &= \frac{1}{N} \sum_{k=1}^N e^{j\omega T_{k1}} Y_k(\omega) \\ &= \sum_{k=1}^N H_{1k}^{(1)}(\omega) Y_k(\omega), \end{aligned} \quad (A-2)$$

where $H_{1k}^{(1)}(\omega) = \frac{1}{N} e^{j\omega T_{k1}}$.

The first estimate of S_2 is defined in terms of the residuals

$$\{Y_k(\omega) - \hat{S}_1^{(1)}(\omega) e^{-j\omega T_{k1}}\}_{k=1}^N:$$

$$\begin{aligned} \hat{S}_2^{(1)} &= \frac{1}{N} \sum_{k=1}^N e^{j\omega T_{k2}} \left[Y_k(\omega) - \frac{1}{N} \sum_{\ell=1}^N Y_\ell(\omega) e^{j\omega(T_{1\ell} - T_{k1})} \right] \quad (A-3) \\ &= \sum_{k=1}^N H_{2k}^{(1)}(\omega) Y_k(\omega), \end{aligned}$$

where $H_{2k}^{(1)} = \frac{1}{N} [e^{j\omega T_{k2}} - \frac{1}{N} A^*(\omega) e^{j\omega T_{k1}}]$.

Note that $A = \sum_{k=1}^N e^{j\omega(T_{k1}-T_{k2})}$ as defined by Shumway (1972).

The second estimate of S_1 is defined as a beam on the residuals

$$\{Y_k(\omega) - \hat{S}_2^{(1)}(\omega) e^{-j\omega T_{k2}}\}_{k=1}^N:$$

$$\hat{S}_1^{(2)} = \frac{1}{N} \sum_{k=1}^N e^{j\omega T_{k1}} [Y_k(\omega) - \sum_{\ell=1}^N H_{2\ell}^{(1)}(\omega) Y_\ell(\omega) e^{-j\omega T_{k2}}] \quad (A-4)$$

$$= \sum_{k=1}^N H_{1k}^{(2)}(\omega) Y_k(\omega),$$

where $H_{1k}^{(2)}(\omega) = \frac{1}{N} [e^{j\omega T_{k1}} - A(\omega) H_{2k}^{(1)}(\omega)]$.

If we rewrite $H_{2k}^{(1)}$ in terms of $H_{1k}^{(1)}$, we obtain

$$H_{2k}^{(1)} = \frac{1}{N} [e^{j\omega T_{k2}} - A^*(\omega) H_{1k}^{(1)}]. \quad (A-5)$$

These recursions are general, and thus, one may write:

$$H_1^{(k+1)} = \frac{1}{N} [U_1 - A H_2^{(k)}] \quad (A-6)$$

and

$$H_2^{(k)} = \frac{1}{N} [U_2 - A^* H_1^{(k)}] \quad (2)$$

$$\text{where } H_i^{(k)} = \begin{bmatrix} H_{i1}^{(k)}(\omega) \\ \vdots \\ H_{iN}^{(k)}(\omega) \end{bmatrix} \quad \text{and} \quad U_i = \begin{bmatrix} e^{j\omega T_{1i}} \\ \vdots \\ e^{j\omega T_{Ni}} \end{bmatrix}$$

Note that $A = U_2^+ U_1$.

Combining (1) and (2), we obtain:

$$\begin{aligned} H_1^{(k+1)} &= \frac{1}{N} [U_1 - \frac{1}{N} A(U_2 - A^* H_1^{(k)})] \\ &= \frac{1}{N} [U_1 - \frac{1}{N} A U_2] + \frac{1}{N^2} |A|^2 H_1^{(k)}. \end{aligned} \quad (A-7)$$

It can be shown that this sequence converges geometrically to

$$H_1^{(\infty)} = \frac{N^{-1} [U_1 - N^{-1} A U_2]}{1 - N^{-2} |A|^2}. \quad (A-8)$$

Further,

$$H_2^{(\infty)} = \frac{N^{-1} [U_2 - N^{-1} A^* U_1]}{1 - N^{-2} |A|^2}. \quad (A-9)$$

Equations (A-8) and (A-9) are seen to be the two-signal maximum-likelihood vector equations (for spatially white noise).

The error estimate after k iterations is given by:

$$\epsilon = \frac{1}{N} O\left[\frac{\rho^{(k+1)}}{1-\rho^2}\right] \quad (\text{A-10})$$

where

$$\rho \doteq N^{-2} |A|^2.$$

Thus, the rate of convergence is a function of the separation of the plane wave vectors of the two signals. In fact, ρ is the normalized correlation between the two vectors.

For comparison, the two-signal maximum-likelihood signal estimates (for spatially white noise) are given as follows (Shumway, 1972):

$$H_{1k} = \Delta^{-1}(\omega) [N e^{j\omega T_{k1}} - A(\omega) e^{j\omega T_{k2}}] \quad (\text{A-11})$$

and

$$H_{2k} = \Delta^{-1}(\omega) [N e^{j\omega T_{k2}} - A^*(\omega) e^{j\omega T_{k1}}],$$

where $\Delta(\omega) = N^2 - |A(\omega)|^2$ and $A(\omega) = \sum_{\ell=1}^N e^{j\omega(T_{\ell 1} - T_{\ell 2})}$.

Then:

$$S_1(\omega) = \sum_{k=1}^N H_{1k}(\omega) Y_k(\omega) \quad (A-12)$$

$$S_2(\omega) = \sum_{k=1}^N H_{2k}(\omega) Y_k(\omega).$$

APPENDIX II

Discussion of Bias in an Alternative Iterative
Signal Processor

To see that bias exists in the signal estimate obtained in the alternative manner discussed in the beginning of the text of this report, consider the following mixed-signal model for a two-channel array:

$$y_1(t) = s_1(t-T_{11}) + s_2(t-T_{12})$$

$$y_2(t) = s_1(t-T_{21}) + s_2(t-T_{22}).$$

Let us assume that we desire a signal estimate for Event 1, but that we will beam first on the epicenter for Event 2:

$$\hat{s}_2(t) = s_2(t) + \frac{1}{2}[s_1(t-T_{11}+T_{12}) + s_1(t-T_{21}+T_{22})].$$

This is the 0'th iteration for signal 2. Shifting and subtracting this estimate to eliminate signal 2 from the original recordings ($y_1(t)$ and $y_2(t)$), and then beaming on Event 1 yields the signal estimate

$$s_1(t) = s_1(t) - \frac{1}{4}[2s_1(t) + s_1(t-T_{21}+T_{22}+T_{11}-T_{12}) + s_1(t+T_{21}-T_{22}-T_{11}+T_{12})].$$

We see that this estimate for signal 1 is distorted only by echos of itself. Further, it contains a predictable, on-beam contribution from signal 1 which

reduces the scale of the signal estimate; thus, the estimate is biased. Here, this component has a value of $-\frac{1}{2} s_1(t)$. In general, we believe that the predictable bias is given by:

$$\left[-N(2N-1)^{(m-1)/2} \right] \left[N^{-m-1} \right] s_i(t)$$

where N is the number of channels, m is an odd number ($m=2p-1$, where p is the iteration number), and $s_i(t)$ is the signal estimated at the middle of the iteration. This formula has not been formally derived, but is correct for all cases we have worked out, including $N=2$, $m=1,3,5,7$; $N=3,4$, $m=1,3$; and $m=1$, all N .

At the end of the first iteration, the signal estimate for Event 2 again is of the form:

$$\hat{s}_2(t) = s_2(t) + f[s_1(t)].$$

The above results suggest that the signal estimates extracted at the middle of an iteration will converge slowly. As such, it would appear that the proper mode for implementation of the iterative-beam processor if one desires an accurate signal estimates is to beam first on the signal of interest, and to use only those signal estimates produced at the end of each iteration.